OVERAL PERFORMANCE PREDICTION OF TURBO ROTARY COMPOUND (TURC) ENGINE USING SIMULATION RESULTS OF ENGINE COMPONENTS

A THESIS SUBMITTED TO
THE GRADUATE SCHOOL OF NATURAL AND APPLIED SCIENCES
OF
THE MIDDLE EAST TECHNICAL UNIVERSITY

BY

MEHMET KARACA

IN PARTIAL FULFILLMENT OF THE REQUIREMENTS
FOR
THE DEGREE OF MASTER OF SCIENCE
IN
THE DEPARTMENT OF AEROSPACE ENGINEERING

JULY 2005

Approval of the Graduate School of Natural and Applied Sciences

____
Prof.Dr. Canan ÖZGEN
Director

I certify that this thesis satisfies all the requirements as a thesis for the degree of Master of Science

____
Prof.Dr. Nafiz ALEMDAROĞLU
Head of Department

This is to certify that we have read this thesis and that in our option it is fully adequate, in scope and quality, as a thesis for the degree of Master of Science.

____
Prof. Dr. İ. Sinan AKMANDOR
Supervisor

Examining Committee Members

Prof. Dr. Yusuf ÖZYÖRÜK (METU,AEE)_______________________

Prof. Dr. İ. Sinan AKMANDOR (METU,AEE)_______________________

Ins. Tahsin ÇETİNKAYA (METU,ME)_______________________

Asoc. Prof. Dr. Ozan TEKİNALP (METU,AEE)_______________________

Asoc. Prof. Dr. Serkan ÖZGEN (METU,AEE)_______________________

ABSTRACT

OVERAL PERFORMANCE PREDICTION OF TURBO ROTARY COMPOUND ENGINE (TURC) USING SIMULATION RESULTS OF ENGINE COMPONENTS

Karaca, Mehmet
M. S., Department of Aerospace Engineering
Supervisor : Prof. Dr. İ. Sinan Akmandor

JULY,2005 59 Pages

The thesis proposes an overall performance estimation procedure for a new turbo-rotary compound engine (TURC) and an associated novel thermodynamic cycle. In this engine, two or multiple spools are lined up in series within the engine. In the front spool, positive displacement rotary vane type turbines drive axial compressor the performance of which were estimated using stage stacking calculations. In the back spool, axial turbine stages drive positive displacement rotary vane type compressors, the performance of axial turbine was predicted by series matching of turbine stages. Two air streams feed separately the customary turbo components and the rotary vane components, respectively. Accordingly, the primary high mass flow through the axial compressors and turbines undergoes Bryton cycle, where as the secondary, low mass flow through the positive displacement rotary components is mainly undergoes Akmandor cycle, which is a novel thermodynamic cycle. The energy consumed internally by the engine is minimized because less input shaft power is needed for the rotary vane compressors and higher inlet temperatures and less cooling can be tolerated by the intermittent combustion rotary vane turbines. The result is a radical improvement in both efficiency and net power output. But this result can be estimated, since the novel engine is the combination of a high efficiency internal combustion engine and high performance gas turbine engine. Aerothermodynamics and spool matching calculations comparing a T56-A14 core with a TURC of similar size and compression ratio show that the new engine provides superior performance characteristics by increasing the net output work by 100% and decreasing the specific fuel consumption by 20%.

Keywords: Performance, Matching, Compressor, Turbine, Rotary Vane Engine, Compound Engine, Turbomachinery, Performance Map.

ÖZ

MOTOR BİLEŞENLERİNİN BENZETİŞİM SONUÇLARINI KULLANARAK TURBO DÖNER BİLEŞİMLİ BİR MOTORUN (TURC) TOPLU PERFORMANS TAHMİNİ

Karaca, Mehmet
Yüksek Lisans, Havacılık ve Uzay Mühendisliği Bölümü
Tez Yöneticisi: Prof. Dr. İ. Sinan Akmandor

TEMMUZ 2005, 60 Sayfa

Bu tezde, yeni bir turbo-döner bileşimli motor (TURC) için performans öngörü prosedürü ile bu motor için yeni bir termodinamik çevrim sunulmaktadır. Sözü edilen motorda, iki ya da daha fazla şaft motor boyunca seri olarak sıralanmaktadır. Ön şaftta, döner vana tipli kısmî giriş türbinleri kademe bindirme yöntemiyle performansı hesaplanan eksenel compressor kademelerini kontrol eder. Arka şaftta ise, performans özellikleri seri eşleme ile tahmin edilen eksenel türbin, kademeleri döner tipli kısmî giriş kompresörlerini kontrol etmektedir. Klasik turbo bileşenleri

ile döner vana bileşenlerini iki ayrı hava akımı besler. Buna uygun olarak, eksenel kompresör ve türbinlerden geçen yüksek kütleli birincil akım, Bryton döngüsünde iken, kısmî giriş döner bileşenlerden geçen düşük kütleli ikincil akım ise, yeni ve patentli bir döngü olan Akmandor döngüsündedir. Döner vanalı kompresörler için daha düşük giriş mil gücü kullanıldığından ve döner vanalı türbinlerin, aralıklı yapısıyla, yüksek giriş sıcaklıkları ile yetersiz soğutma durumlarına karşı daha toleransı olmasından dolayı, motor tarafından içerde tüketilen enerji miktarı minimuma çekilmektedir. Sonuç, hem verim hem net güç çıktısı açısından radikal bir ilerlemeyi gösterir. Ancak sözü edilen motorun yüksek verimli içten yanmalı bir motorla yüksek performans özellikleri olan bir gaz türbinin birleşimi olduğu düşünüldüğünde bu beklenilen bir sonuçtur. T56-A14 iç gövdesinin aynı boyut ve sıkıştırma oranındaki bir TURC ile karşılaştırıldığı, aerotermodinamik ve makara eşleme hesapları, yeni motorun oldukça yüksek performans özelliklerine sahip olduğunu göstermektedir. Yakıt tüketiminde %20'lik bir azalmaya karşılık net iş çıktısında %100'lük bir artış gözlenir.

Anahtar Kelimeler: Performans, Eşleme, Kompresör, Türbin, Döner Bileşimli Mototr, Birleşik Motor, Turbomakine, Performans Haritası.

I hereby declare that all information in this document has been obtained and presented in accordance with academic rules and ethical conduct. I also declare that, as required by these rules and conduct, I have fully cited and referenced all material and results that are not original to this work.

Mehmet KARACA

ACKNOWLEDGMENTS

I would like to express my sincere appreciation to my thesis supervisor Prof. Dr. İ. Sinan AKMANDOR for his invaluable supervision, guidance and insight throughout the study and as well as my carier.

I express my sincere to Prof. Dr. Yalçın GÖĞÜŞ and his colleague Murat ARSLANOĞLU for their study on performance prediction which is a base for my thesis.

TABLE OF CONTENTS

LIST OF TABLES

TABLE

LIST OF FIGURES

FIGURES

LIST OF SYMBOLS

Q Heat (2.1)

W Work (2.1)

U Internal Energy (2.1)

E Total Energy

H Enthalpy

C_p Constant Pressure Specific Heat

C_v Constant Volume Specific Heat

T Temperature

u Internal Energy

p Pressure

q Specific Heat

w Specific Work

γ Specific Heat Ratio.

R Gas Constant

n Polytropic Index (2.1)

ρ_{in} Inlet Air Density

V_{in} Inlet initial volume of positive displacement components

N Rotational Speed (RPM)

HP_C Compressor Power

HP_t Turbine Power

ϕ Flow Coefficient

V_a Axial Velocity

U Tangential Velocity at Mean Radius

Ψ Pressure Coefficient.

t_i Stage Inlet Temperature.

π_s Stage Pressure Ratio

ζ Temperature Rise

η_s Stage Efficiency

Q'_i Mass Flow Parameter at the Inlet of Each Stage.

α_i Flow Angle at Design Point at I th Stage Inlet.

A_{Ni} i th Stage Annulus Area

M_i i th Stage Inlet Mach Number.

N Rotational Speed (RPM)

r_{mi} i th Stage Mean Radius

π Overall Pressure Ratio

η Overall Efficiency

λ Work-speed Correlation Parameter

PR Pressure Ratio

ε $(\gamma-1)/\gamma$

ECV Effective Calorific Value of Combustor Fuel

P_{TO} Overall Pressure Ratio

K_{in} Inlet Pressure Loss Coefficient

η_m Mechanical Efficiency

PF Penalty Factor for the Cost Function

E_i i th Error Term

η_c Compressor Efficiency

η_t Turbine Efficiency

γ_c Compressor Specific Heat Raito

γ_t Turbine Specific Heat Ratio

SFC Specific Fuel Consumption

CHAPTER 1

INTRODUCTION

1.1 Objective

Since 1930's starting from Frank Whittle's Von Ohain's prototype, gas turbines have spread out on the world. Meanwhile, gas turbine technology has improved rapidly especially at early stages of invention. But today, "this technology is very mature and the improvements comes only as small innovations at the expense of very hard work. Widespread usage area of gas turbines makes this innovations very crucial"[30].

High specific power and long maintenance periods of the gas turbines makes them indispensable at high peak power demands, but for small power ranges, even the most efficient gas turbines can not reach the efficiency of the otto cycle engines. Compound engines combining the advantages of gas turbines and otto cycle would seem promising, therefore, there has been a significant number of studies on compound engine modelling.

Gas generator is the core of the gas turbine and is composed of compressor turbine and combustion chamber lined upon the shaft. Consequently, estimation of the performance of the gas generator at design and off-design is cruicial for understanding the overall behaviour of the gas turbine.

In the preliminary or conceptional design phases of any new gas turbine engine project, the design and off design performance prediction is a major prerequisite. The focus shall be set mainly on understanding the behaviour of turbomachinery components for the performance prediction of the drafted engine over full range of operating conditions.

It’s possible to design individual components of a gas turbine so that the engine will give the required performance at design point with simple calculations.

The main problem is the variation of performance over complete operating range also referred to as off design performance. The operation range of components will further be reduced when they are part of a gas turbine engine.

The variation of power for different ambient conditions is important for an arbitrary industrial gas turbine hot summer days means maximum

There are many simulation studies for the prediction of the performance of gas turbines. Computer simulation codes are the common tools for the estimation of the performance of the gas turbine engines.

The purpose of the study was to establish a simulation technique for the aerothermodynamic performance of a novel turbo rotary compound engine and the comparison of the performance analysis results with a commercial gas turbine.

1.2 Methodology of Engine Performance Estimation

The performance of the gas generator spool depends on the behaviour of its main components turbine, compressor and combustion chamber. In order to estimate the performance of a particular engine, the characteristic data of rotating components must be correct and accurate enough. In this study since one dimensional conservation equations are used for turbo components, the detailed geometries of individual stages of the turbo components are not needed. However, in order to simulate the aerothermodynamic behaviour of the turbo components, the generalized stage characteristic curves are needed for turbo compressor and turbine. For positive displacement components, the compression and expansion processes are assumed to be polytropic.

“The performance of a turbo compressor is normally affected by the total pressure ratio, corrected mass flow rate, corrected engine speed and component efficiency. Most ofen this performance is presented in one map showing the interrelationship of all these parameters. Sometimes, for clarity, two maps are used, with one showing the pressure ratio versus corrected mass flow rate/corrected speed (Figure 1.1) and the the other showing compressor efficiency versus corrected mass flow rate/corrected speed."[3]

The turbo compressor performance map can be constructed from stage level, using a set of non-dimensional stage characterisics such as pressure rise and temperature loading as a function of flow coefficient. The stage stacking procedure described in Figure (2.8) has been used. At each point on the performance data, compatibility of mass flow, temperature and pressure values between adjacent stages is sought.

The flow through a turbo turbine first passes through stationary airfoils which turn and accelerate the fluid, increasing its tangential momentum. The flow then goes around rotating airfoils that remove its energy as they change its tangential momentum. Successive pairs of stationary airfoils remove additional energy from the fluid. To obtain a high output power to weight ratio from a turbine, the flow entering first-stage turbine rotor is usually close to supersonic which requires the flow to pass through a choked turbine nozle area. This flow characteristics is shown in the typical turbine performance map.

The performance of a turbine is plotted in terms of total pressure ratio, corrected mass flow rate, corrected turbine speed, and component efficiency. This performance can be represented in two maps or a combined map. when two maps are used, one map shows the interrelationship of the total pressure ratio, corrected mass flow rate, and corrected turbine speed, like the one depicted in figure 1.2. The other map shows the interrelationship of turbine efficiency versus corrected mass flow rate/expansion ratio, like the one shown in Figure 1.3 This spreads out the lines of corrected speeds and the turbine efficiency can now be shown.

The turbine performance map is estimated by a procedure similar to the compressor map synthesis technique. The major steps are

1. The single stage modelling using design point data and the generalized stage data,
2. Series matching of individual stages.

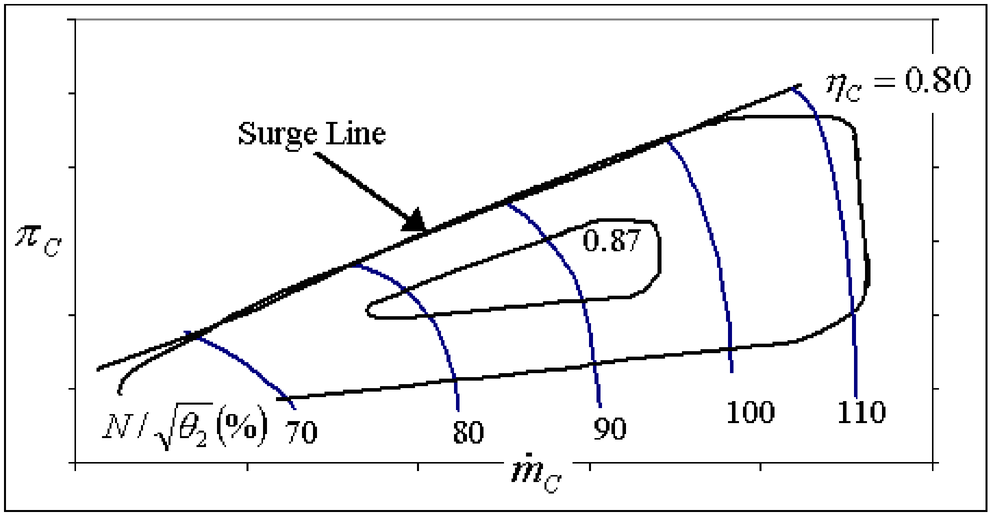

Figure (1.1) Typical Compressor Performance Map.

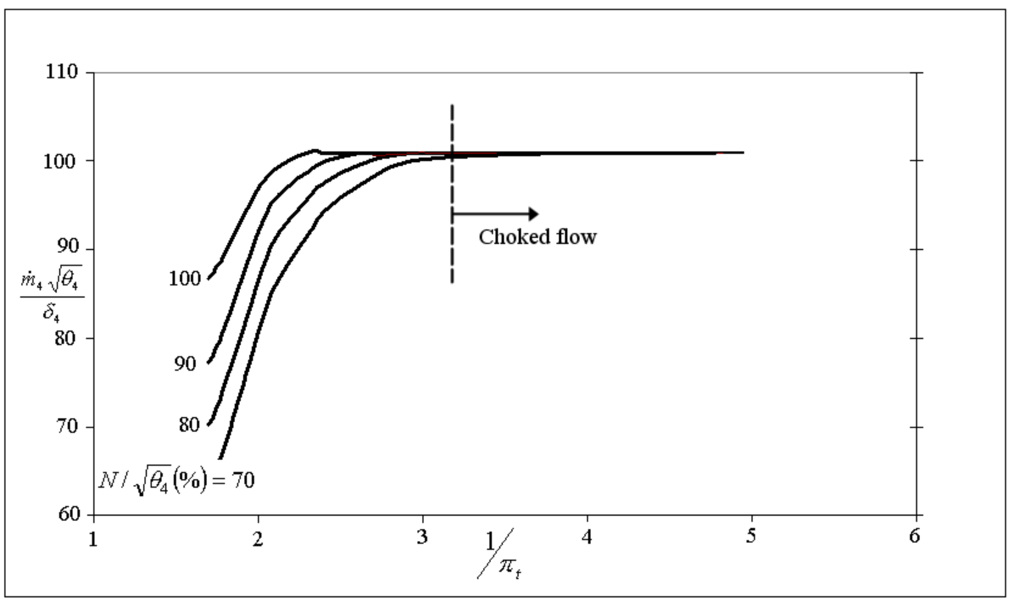

Figure (1.2) Typical Turbine Flow Map.

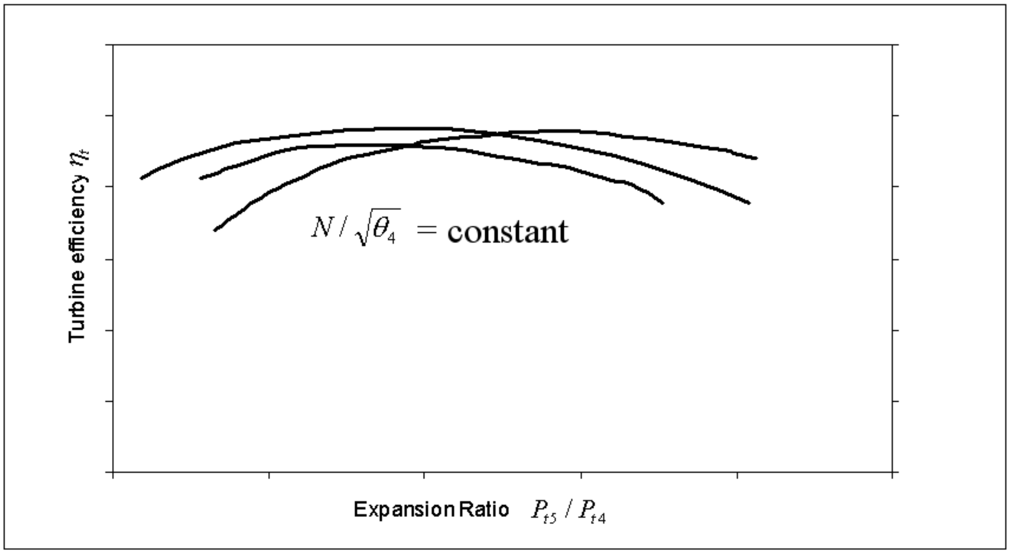

Figure (1.3) Typical Turbine Efficiency Map.

1.3 Turbo Rotary Compound Engine

The study purposes to investigate the performance of the novel Turbo Rotary Compound (TURC) Engine. In this engine shafts linking customary gas turbine engines components such as axial compressor and axial turbines are eliminated. Instead two or multiple spools are lined up in series within the engine.

The present study proposes a new compound type engine turbo-rotary compound engine (TURC) with associated novel thermodynamic cycle (Figure 1.4). In this engine, shafts linking customary gas turbine engines components such as axial compressors and axial turbines are eliminated. Instead, two or multiple spools are lined up in series within the engine (Figure 1.5). In the front spool, partial admission rotary vane type turbines drive axial compressor stages. In the back spool, axial turbine stages drive partial admission rotary vane type compressors. “Two air streams feed separately the customary turbo components and the rotary vane components, respectively. Accordingly, the primary high mass flow through the axial compressors and turbines is mainly responsible for the generation of net engine thrust and power, where as the secondary, low mass flow through the positive displacement rotary components is mainly used to generate the internal energy required to power the axial compressor stages. The energy consumed internally by the engine is minimized because less input shaft power is needed for the rotary vane compressors and higher inlet temperatures and less cooling can be tolerated by the intermittent combustion rotary vane turbines."[3]

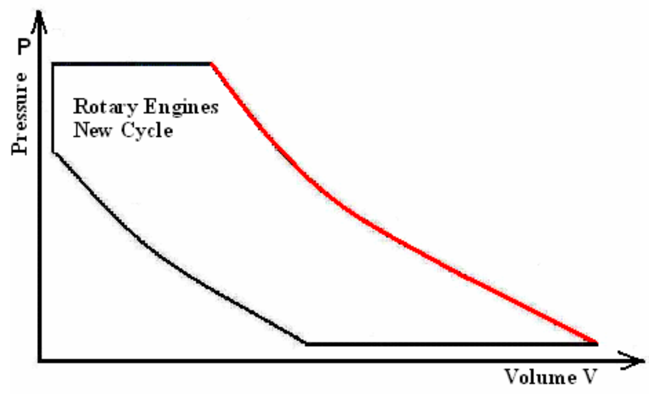

Figure (1.4) Thermodynamic Cycle of Rotary Engine.

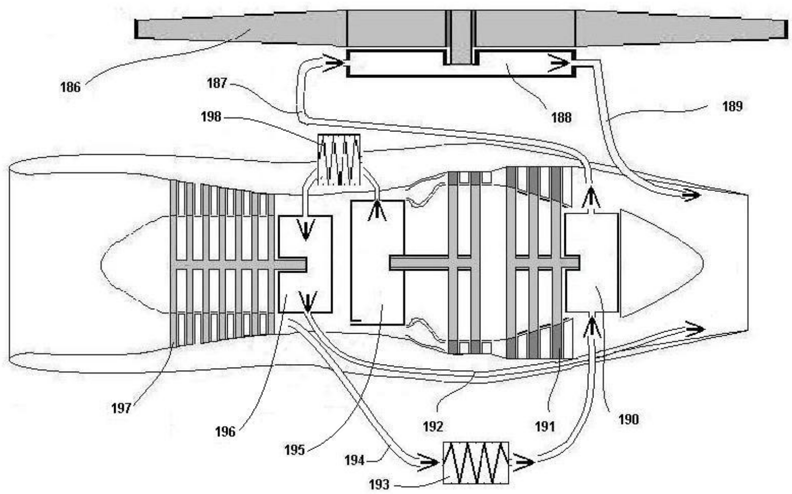

Figure (1.5) Schematic diagram of Turbo-Rotary Compound Engine [27].

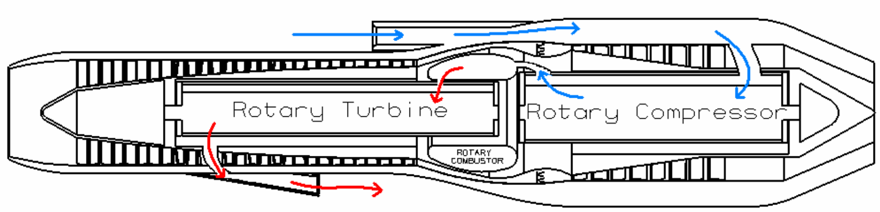

Figure (1.6) Visual Schematic diagram of Turbo-Rotary Compound Engine.

1.4 Outline of the Thesis

In the preceding thesis [2], performance estimation model developed by GasTOPs Ltd. [1] used for modelling single shaft gas turbine was presented, while and an improved model developed for overall performance estimation of novel compound TURC engine was explained. The results obtained through the performance estimation computer programs were compared.

Individual performance characteristic estimation models for all rotary components are explained in Chapter 2. First, the model used for the positive displacement compressor and turbine explained. Then, Secondly, performance map estimation model for turbo compressor explained and the resulting performance maps are tabulated. Finally turbo turbine performance map estimation procedure is explained and results are tabulated.

The method of overall performance estimation, using cycle analysis modelling the gas turbine as combination of modules is explained in Chapter 3. The component modules of turbo positive displacement and combustor are explained briefly. Finally, the method of multivariable search Simplex Method was explained in Chapter 3.

In Chapter 4 the results of overall performance estimation procedure for several runs for both T56-A14 and Turbo Rotary Compound Engine are tabulated. The resulting figures include the operation ranges, efficiencies, Fuel Consumption etc.. Comparative interpretation of the results listed in Chapter 4 are given in the Chapter 5.

CHAPTER 2

COMPONENT PERFORMANCE SIMULATION

In order to simplify the performance estimation problem, the operating cycle of the engine is broken into sequence of processes. Individual mathematical models developed for each engine components can be at various levels of approximation[8]. By combining the performance estimation results of each component, the overall engine performance is obtained

In this Chapter, the simulation of the rotary components (both turbo and positive displacement) are presented. In the first part a brief summary of the thermodynamic relations are given (Explained at Reference [7]). Then the positive displacement component model is explained. Finally, the turbo component performance estimation presented.

2.1 Governing Equations

Various forms of energy are can be classified as heat Q, work W, and total energy E. Mathematically the first law of thermodynamics is can be expressed as

$$Q - W = \Delta E \qquad (2.1)$$

where,

Q = net heat transfer across system boundaries.

W = net work done in all forms.

ΔE = net change in the total energy of the system.

Net Energy to (or from) the system as heat and work.	=	Net increase (or decrease) in the total energy of the system.

The equation in differential form is,

$$\delta Q - \delta W = dE \tag{2.2}$$

The energy E may include many forms of energies like kinetic energy, potential energy, internal energy etc. but for stationary closed systems internal energy that is due to change in temperature alone is the most important. It is denoted by U and the firs law is written as [6]:

$$Q - W = \Delta U \tag{2.3}$$

Constant Volume Isochoric Process is encountered in the analysis of air standard cycles like Otto, Diesel and also the Amador cycle which is the thermodynamic cycle of positive displacement flow of the hybrid Truce engine [28]. The initial combustion of the flow through positive displacement components is an isochoric process.

If there is no change in the volume, the work $\int(pdV)$ is zero. Then, according to the first law for the constant volume process the change in the internal energy is equal to the heat transfer,

$$dU = \delta Q = mC_v dT = mC_v(T_2 - T_1)$$

(2.4)

As the name implies constant pressure or isobaric process, is a steady non-flow processes where that the pressure does not change (i.e. isobaric). The final combustion of the flow through positive displacement components and combustion in the flow through turbo components assumed to be almost isobaric (pressure loss). Then,

$$\delta Q = dU + pdV = d(U + pV) = dH \tag{2.5}$$

where H is known as the enthalpy. Consequently, during a constant pressure process, heat transfer is equal to change in enthalpy or;

$$dH = \delta Q = mC_p dT \tag{2.6}$$

The isothermal process on a p-V diagram is illustrated in Figure 2.1. Since there is no temperature change during this process, there will not be any change in internal energy (i.e., du = 0), then according to the firs law [7].

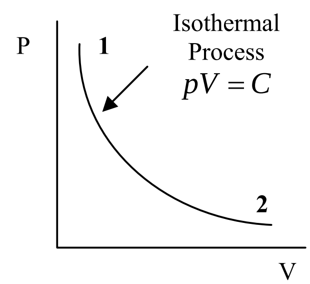

Figure (2.1) Isentropic Process

$$\delta Q = \delta W \tag{2.7}$$

or

$$Q_{1-2} = \int_1^2 pdV = p_1 V_1 \log_e \left(\frac{V_2}{V_1} \right) \tag{2.8}$$

If a process occurs in such a way that there is no heat transfer between the surroundings and the system, but the boundary of the system moves giving displacement work, the process is said to be adiabatic. Such a process is possible if the system is thermally insulated from the surroundings [7].

Hence, $\delta Q = 0$,therefore,

$$\delta W = -\delta U = -mC_v dT \tag{2.9}$$

Reversible adiabatic process is also known as isentropic process. Let $pV^{\gamma} = C$ be the mathematical relation representing isentropic process. For unit mass flow,

$$q_{1-2} = 0 = w_{1-2} + u_2 - u_1 \tag{2.10}$$

or

$$w_{1-2} = -(u_2 - u_1) \tag{2.11}$$

In other words, work is done at the expense of internal energy

$$W_{1-2} = \int_1^2 pdV = \int_1^2 \frac{C}{V^{\gamma}} dV \tag{2.12}$$

$$= \frac{\left[CV^{1-\gamma}\right]_{V1}^{V_2}}{1-\gamma} \tag{2.13}$$

$$= \frac{CV_2^{\ 1-\gamma} - CV_1^{\ 1-\gamma}}{1-\gamma} \tag{2.14}$$

When $C = p_1 V_1^{\gamma} = p_2 V_2^{\gamma}$,

$$W_{1-2} = \frac{p_2 V_2^{\gamma} V_2^{1-\gamma} - p_1 V_2^{\gamma} V_2^{1-\gamma}}{1-\gamma} \tag{2.15}$$

$$= \frac{p_1 V_1 - p_2 V_2}{1-\gamma} \tag{2.16}$$

Using p_{ave}=RT for unit mass flow we have,

$$w_{1-2} = \frac{R(T_1 - T_2)}{\gamma - 1} \tag{2.17}$$

$$= C_v (T_1 - T_2) = -(u_2 - u_1) \tag{2.18}$$

$$\frac{p_1 V_1}{T_1} = \frac{p_2 V_2}{T_2} \tag{2.19}$$

therefore,

$$\frac{T_2}{T_1} = \frac{p_2 V_2}{p_1 V_1} = \left(\frac{V_1}{V_2}\right)^{\gamma}\left(\frac{V_2}{V_1}\right) = \left(\frac{V_1}{V_2}\right)^{\gamma-1} \tag{2.20}$$

$$\frac{T_2}{T_1} = \frac{p_2 V_2}{p_1 V_1} = \left(\frac{p_1}{p_2}\right)^{\frac{1}{\gamma}}\left(\frac{p_2}{p_1}\right) = \left(\frac{p_2}{p_1}\right)^{\left(\frac{\gamma-1}{\gamma}\right)} \tag{2.21}$$

$$\frac{T_2}{T_1} = \left(\frac{V_1}{V_2}\right)^{\gamma-1} = \left(\frac{p_2}{p_1}\right)^{\left(\frac{\gamma-1}{\gamma}\right)} \tag{2.22}$$

In polytropic process, both heat and work transfers take place. It is denoted by the general equation $pV^n = C$, where n is the polytropic index. For the positive displacement compressor and turbine model is developed assuming processes are polytropic. The following equations for the reversible adiabatic process which is only a special case of polytropic process with $n = \gamma$.[7]

$$p_1 V_1^n = p_2 V_2^n \tag{2.23}$$

$$\frac{T_2}{T_1} = \left(\frac{V_1}{V_2}\right)^{n-1} \tag{2.24}$$

$$\frac{T_2}{T_1} = \left(\frac{p_2}{p_1}\right)^{\left(\frac{n-1}{n}\right)} \tag{2.25}$$

and

$$w_{1-2} = \frac{p_1 V_1 - p_2 V_2}{1-\gamma} \tag{2.26}$$

The above processes are summarized in Table (2.1)

Process	Index N	p, V, T relation	Heat Transfer	Work $\int pdV$	Work $\int pdV$	ΔU
Constant Volume		$T_1 / T_2 = V_1 / V_2$	$mC_v(T_2 - T_1)$	**0**	$V(p_2 - p_1)$	$mC_v(T_2 - T_1)$
Constant Pressure	**0**	$T_1 / T_2 = V_1 / V_2$	$mC_p(T_2 - T_1)$	$p(V_2 - V_1)$	**0**	$mC_v(T_2 - T_1)$
Isothermal	**1**	$p_1V_1 = p_2V_2$	$p_1V_1 \log_e\left(\frac{V_2}{V_1}\right)$	$p_1V_1 \log_e\left(\frac{V_2}{V_1}\right)$	$p_1V_1 \log_e\left(\frac{V_2}{V_1}\right)$	**0**
Isentropic	**γ**	$p_1V_1^\gamma = p_2V_2^\gamma$ $\frac{T_2}{T_1} = \left(\frac{V_1}{V_2}\right)^{\gamma-1} = \left(\frac{p_2}{p_1}\right)^{\left(\frac{\gamma-1}{\gamma}\right)}$	**0**	$\frac{p_1V_1 - p_2V_2}{1-\gamma}$	$\frac{\gamma}{\gamma-1}(p_2V_2 - p_1V_1)$	$mC_v(T_2 - T_1)$
Polytropic	**n**	$p_1V_1^n = p_2V_2^n$	$\left(\frac{\gamma-n}{1-n}\right)mC_v(T_2 - T_1)$	$\frac{p_1V_1 - p_2V_2}{1-n}$	$\frac{n}{n-1}(p_2V_2 - p_1V_1)$	$mC_v(T_2 - T_1)$

Table (2.1) Summary of Process Relations for Perfect Gas [7]

2.2 Positive Displacement Component Performance Model

"Since the start of the industrial revolution, the reciprocating piston engine based on the Otto and Diesel cycles and, the gas turbine engine based on the Bryton cycle, have largely dominated the market [10]. Despite this fact, for many years, patents on rotary combustion engines [11, 12, 13, 14, 15] have claimed that rotary engines possess many advantages over reciprocating engines such as having high torque, fewer parts, lower weight and fewer reciprocating imbalance. Furthermore, the rotational speed of the rotary compressors and turbines can be higher than piston engines mechanically, this means higher mass flow rate and higher specific power. Although heat engines have received little industrial attention, for over 5 decades, sliding vane rotary compressors have taken an important place in general engineering applications, especially in the capacity range of 10-1000 cc/sec and for delivery pressures in the range of 2-18 bars." [9]

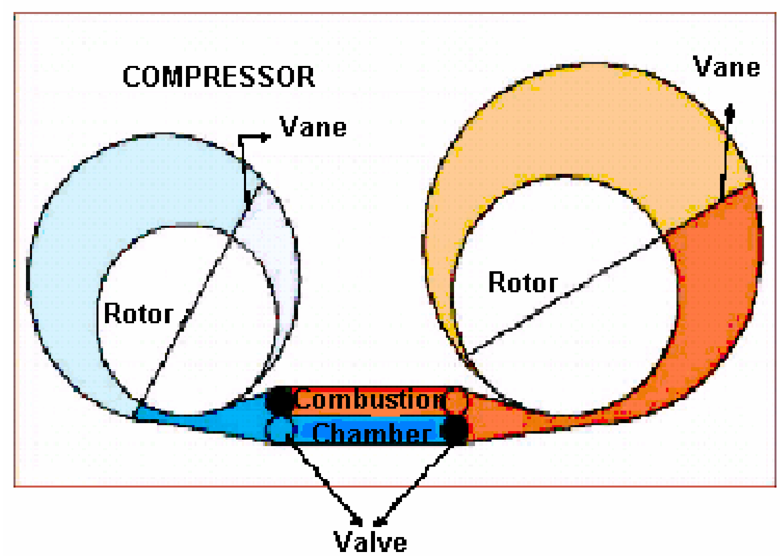

Figure (2.2) Rotary Positive Displacement Components [9]

2.2.1 Positive Displacement Rotary Compressor Model

The mathematical model of the engine was developed like an ordinary internal combustion engine. The compression and expansion processes are assumed to be polytrophic, and the governing equations of the model for these components are given below.

As mentioned above the rotary compressor process is assumed to be polytrophic, constant n for compressor taken to be 1.45. The temperature ratio is evaluated with eon (2.25) and compressor exit temp is,

$$T_2 = T_1 \cdot \left(\frac{p_2}{p_1} \right)^{\left(\frac{n-1}{n} \right)} \qquad (2.27)$$

subscripts 2,1 represent compressor exit and inlet respectively.

The work done on the compressor is calculated as follows

$$HP_c = C_{\_} m C_v \left(T_2 - T_1 \right) \qquad (2.28)$$

The flow through the positive displacement component is calculated as,

$$W = 2 \rho_{in} V_{in} N \qquad (2.29)$$

Assume i_n is constant for compressor

$$W = 2 \cdot C_{\_} \cdot N \qquad (2.30)$$

The constant is chosen to achieve same flow value with the turbo compressor at design point

2.2.2 Positive Displacement Rotary Turbine Model

The rotary turbine process is also assumed to be polytrophic, constant n for compressor assumed to be 1.35. The temperature ratio is evaluated with eon (2.25) and compressor exit temp is,

$$T_4 = T_3 \cdot \left(\frac{p_4}{p_3}\right)^{\left(\frac{n-1}{n}\right)} \tag{2.31}$$

subscripts 4,3 represent turbine exit and inlet respectively.
The shaft work produced by the turbine is calculated as follows

$$HP_t = C \cdot m \cdot C_v \left(T_4 - T_3\right) \tag{2.32}$$

The flow through the positive displacement component is calculated as,

$$W = 2\rho_3 V_{t-in} N$$

where,

$$\frac{P_1}{P_3} = \frac{\rho_1}{\rho_3} \cdot \frac{R_1}{R_3} \cdot \frac{T_1}{T_3} \tag{2.33}$$

$$\rho_3 = \frac{P_3}{P_1} \cdot \frac{R_1}{R_3} \cdot \frac{T_1}{T_3} \tag{2.34}$$

then $W = 2N \cdot \frac{P_3}{P_1} \cdot \frac{R_1}{R_3} \cdot \frac{T_1}{T_3}$ (2.35)

constant is chosen to achieve same flow value with the turbo turbine at design point

2.3. Axial Flow Turbo Compressor Model

Performance estimation procedure of gas turbines usually based on individual performance characteristics of the engine components. In performance calculation programs turbo components are of major interest. Axial flow compressor and turbine operation behaviours are represented by performance maps, that demonstrate flow conditions for all operating range of components.

The methods employed for turbo component performance map estimation are identical to the methods applied in Reference [1],[2].
“Compressor is the most important and troublesome component, due to the fact that its performance is strongly dependent on the engine rotary speed; maximum efficiency is achieved nearby the critical limits (surge) of the compressor” [16].
The behaviour of compressor is modeled with help of compressor maps. The maps are plot of total pressure ratio versus corrected mass flow rate, for lines of constant corrected speed the lines of constant efficiency can be plot on the same diagram, represent major physical phenomena in compressors.
In order to estimate compressor performance map attention is focused on application of one dimensional method. Since, two or three dimensional analysis methods generally difficult to handle whole compressor.
Various methods are applied to estimate the performance map of compressor using one dimensional conservation equations. Scaling methods use assumption of geometric similarity proposedapplied by Saravanamutto and Mc Isaac [31] have been used to model certain fixed geometry pipeline gas turbines. A new scaling method was also published by Kuroki and Ziegler [30] deriving new scaling rules using statistical analysis.
Methods here also been proposed producing the performance characteristics of individual stages from generalized stage characteristics data to be used to estimate overall compressor performance map.

2.3.1. Stage Characteristics

Stage characteristics of an individual stage of a compressor are represented with two characterisitic curves in terms of following corrected coefficients that are evaluated at the mean line conditions:

Flow Coefficient:

$$\phi = V_a / U \tag{2.36}$$

Pressure Coefficient:

$$\psi = \frac{C_p \cdot t_1 \left(\pi_S^{\frac{\gamma-1}{\gamma}} - 1 \right)}{U^2} \tag{2.37}$$

Temperature Rise:

$$\zeta = \frac{C_p \cdot \Delta t_S}{U^2} \tag{2.38}$$

Efficiency:

$$\eta_S = \psi / \zeta \tag{2.39}$$

It is convenient to normalize the stage presure rise coefficient and efficiency curves to obtain generalized relationships between ψ / ψ_{ref} , η / η_{ref} and ϕ / ϕ_{ref} . The values of ϕ_{ref} somewhat arbitrarily chosen as those corresponding to the maximum efficiency, $\eta_{\max}$ (Figure 2.3)

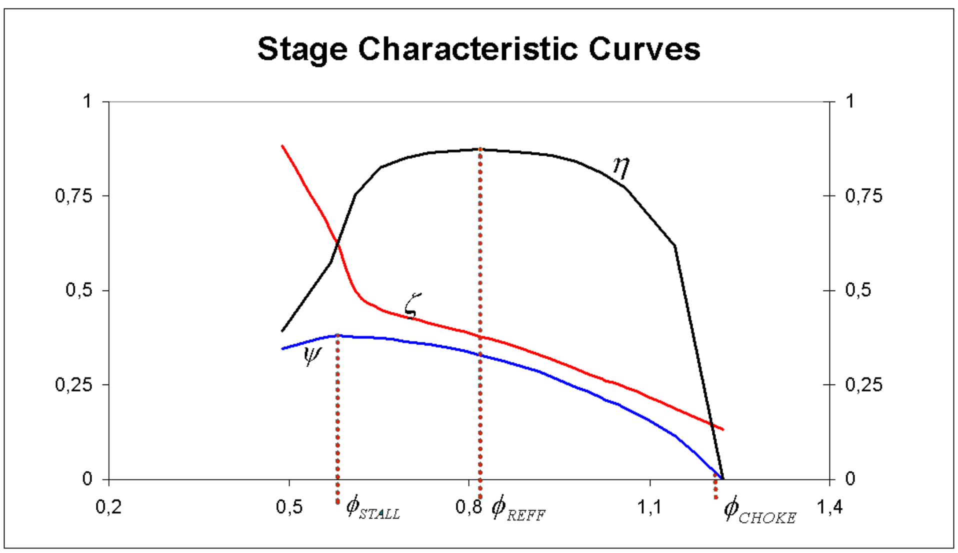

Figure(2.3) Generalized Stage Characteristics.

As well eqn (2.38) follows that

$$\zeta / \zeta_{ref} = \frac{\psi / \psi_{ref}}{\eta / \eta_{ref}} \tag{2.40}$$

Although axial stage characteristics may be estimated analytically using two-dimensional cascade data [29]or three dimensional computational solutions, most engine manufacturers rely on experimental measurements taken in multistage enviroment (compressor rig) to accurately define stage performance.

Plot of ψ / ψ_{ref} vs. ϕ / ϕ_{ref} developed by Gas TOPS Ltd. using stage pressure rise data from number of publications [1,16,17,18,19]. The stage characteristics of T56-A14 used in this study was shown with a curve on the Figure (2.4). A generalized stage efficiency plot developed by Howell [20] is given in Figure (2.5).

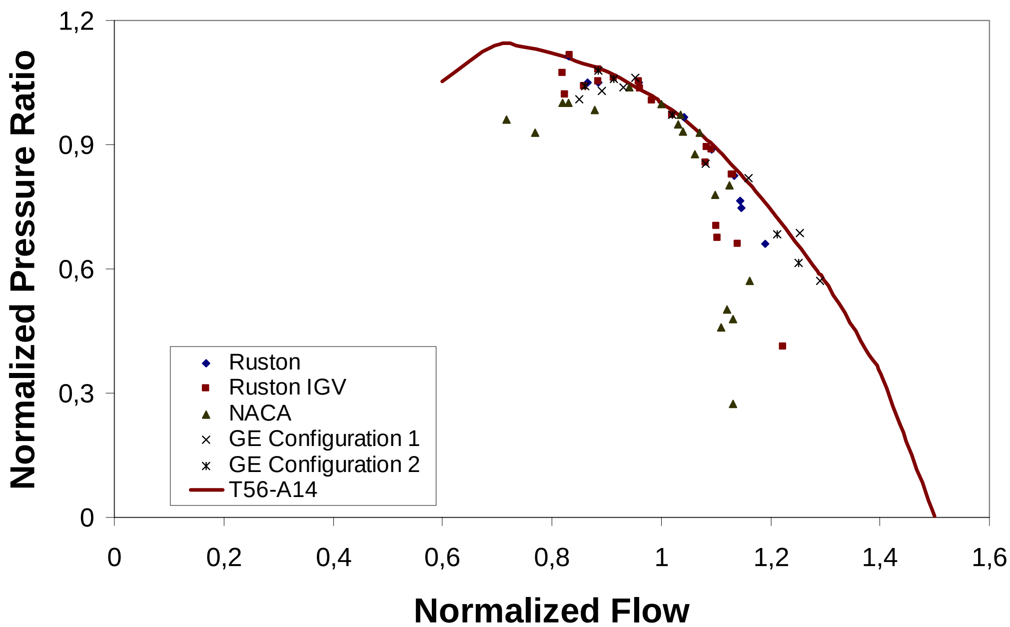

Figure (2.4) Generalized Stage Pressure Rise Coefficient [20]

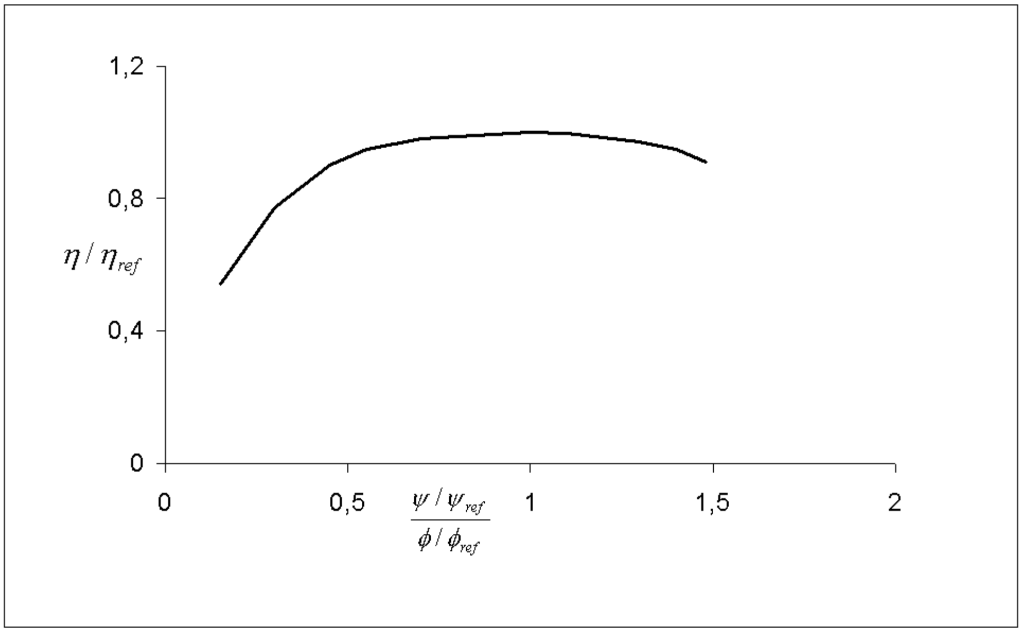

Figure (2.5) Generalized Stage Efficiency Coefficient. [1]

2.3.2 Stage Stacking

Stage stacking is an easy and powerfull tool to deduce compressor performance as soon as the folowing necessary data known correctly:

1. Performance curves of each stage
2. Effective annulus areas at the inlet to each stage, A_{Ni} .Blockage effects due to endwall boundary layer effects are generally included in these areas.
3. Mean radii at inlet of each stage, r_{mi}.
4. Design point values of the absolute flow angle at the inlet to each stage, α_i

Overall compressor performance over a range of speeds and mass flows can be estimated by a so called "stage stacking" method [21,22,23,24]. This is a stage by stage calculation method using the dimensionless stage characteristics for evaluating the pressure ratio and the temperature rise of each stage. After stage by stage calculation overal compressor pressure and temperature rise can be calculated.

The stage stacking procedure is summerized in Figure (2.6)

For assigned values of compressor mass flow, speed, and inlet conditions (p_1,t_1), the first stage flow coefficient is evaluated as follows:

1. Evaluate

$$Q_1' = \frac{W \cdot \sqrt{t_1}}{A_{N1} \cdot \cos\alpha_1 \cdot p_1} \tag{2.39}$$

Where q is the corrected mass flow rate,

$$Q_1' = \sqrt{\tfrac{\gamma}{\Re}}\, M_1 \left(1 + \tfrac{\gamma - 1}{2} M_1^2\right)^{-\frac{\gamma+1}{2(\gamma-1)}} \tag{2.40}$$

By equating (2.39) and (2.40), M_1 can be evaluated by an iterative procedure. Then the stage inlet absolute velocity can be obtained by:

$$\frac{V_1}{\sqrt{t_1}} = M_1 \times \sqrt{\gamma \Re} \tag{2.41}$$

Once V_1 is known, ϕ can be calculated as.

$$\phi = \frac{V_{a1}}{U_1} = \frac{V_1 \cdot \cos\alpha_1}{\left(\frac{2 \cdot \pi \cdot N}{60}\right) \cdot r_{m1}} \tag{2.42}$$

The first stage Φ, in turn i determines the first stage pressure rise and temperature rise coefficients from which the inlet conditions to the second stage are obtained. Thus, in the manner indicated in (Figure 2.6) and using the equations given above, the stage-by-stage calculation is continued throughout the compressor until the performance of each stage das been determined.

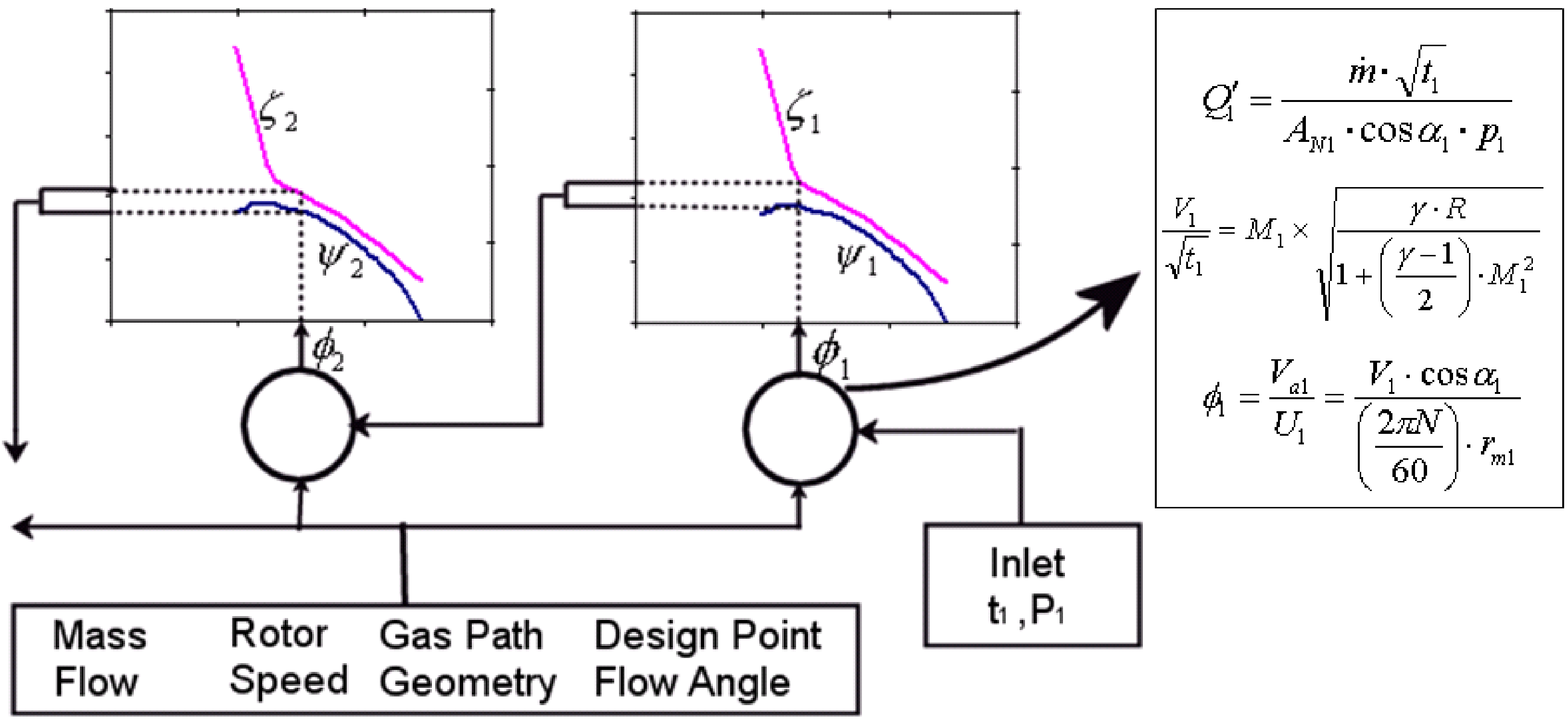

Figure (2.6) Stage Stacking Procedure. [2]

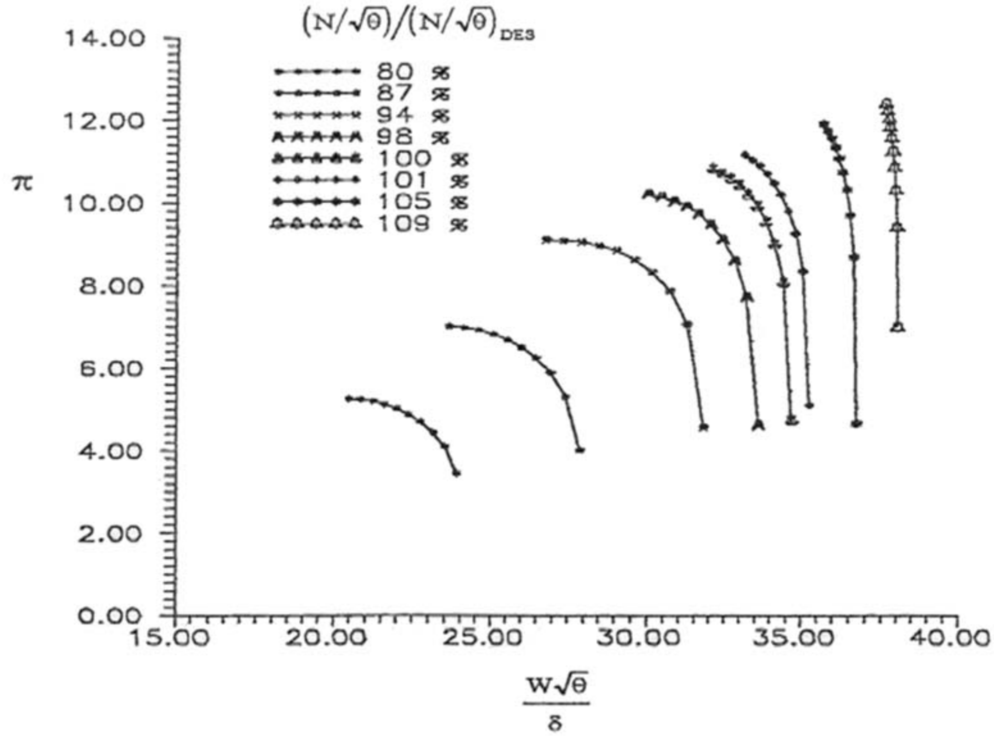

Figure (2.7) T56-A14 Compressor Performance Map [1]

2.4. Axial Flow Turbo Turbine Model

Much of the what has been said for the compressor applies well for the turbines, but two factors lead the major difference between these two turbo component. Firstly, the high temperature at turbine inlet introduces material (structural) problems, leads to lower mach numbers for the turbines and lower tangential mach numbers then the compressor blades of the same radius ease the aerodynamic problem, Secondly, there is pressure drops through the turbine that the boundary layer thiner compared to the compressor. So the aerodynamic design of the turbine is less critical.

A method appiled for the turbine performance estimation is evaluating the total losses as the sum of individual losses, but this method require detailed knowledge of geometry and blading. [25],[26] [1],[2]

Othet method also applied in this study is synthesising overall turbine maps by means of “matching” individual stage data curves that are normalized by stage design performance values. This method is adventageous since the turbine module is treated as a black box that no details of geometry and blading required. The stage performance data can be produced by multivariable search, using available overall performance measurements of turbines designed with simalar design parameters. (blade family, degree of reaction..etc).

The generalized characteristics for T56-A14 turbine stages were developed by GasTOPS Ltd. [1].

The turbine performance map estimation procedure will be summarized. Firstly the performance characteristics of turbine stage used for overall estimation is explained. Then, turbine design point estimation procedure is presented and finally, series matching of turbine stages procedure and the are presented.

2.4.1 Turbine Stage Characteristics

In the present study, performance of turbine stage is represented by two generalized curves developed by gas tops in terms of the following parameters.

Speed:

$$N \Big/ \sqrt{t_{01}} \tag{2.43}$$

Pressure Ratio:

$$\pi = \frac{P_1}{P_2} \tag{2.44}$$

Flow:

$$Q = \frac{W\sqrt{T_1}}{P_1} \tag{2.45}$$

Temperature Drop:

$$\frac{\Delta T}{T} = \frac{T_1 - T_2}{T_1} \tag{2.46}$$

Isentropic Efficiency:

$$\eta = \frac{\Delta T / T}{\left[1 - \left(\frac{1}{\pi}\right)^{\varepsilon}\right]} \tag{2.47}$$

The subscripts 1 and 2, refer to stage inlet and exit conditions respectively.Turbine stage performance characteristics are usually presented with the corrected speed and pressure ratio as the independent variables.

A generalized efficiency correlation is used to demonstrate the off-design efficiency behaviour of a single stage turbines. Especially used to predict the total temperature variation through a single stage turbine (Figure 2.8).

The efficiency is normalized with respect to the design point efficiency of turbine stage plotted against a normalized "work-speed" correlation parameter, where

$$\lambda = \frac{(BladeSpeed)^2}{TurbineSpecificWork}$$

$$\approx \frac{N^2}{\Delta h} \approx \frac{N^2}{\Delta t} \approx \frac{\left(N / \sqrt{t}\right)^2}{(\Delta t / t)} \tag{2.48}$$

The efficiency variation at pressure ratios other than the stage design point pressure ratio is represented by lines of constant corrected pressure ratio lines.

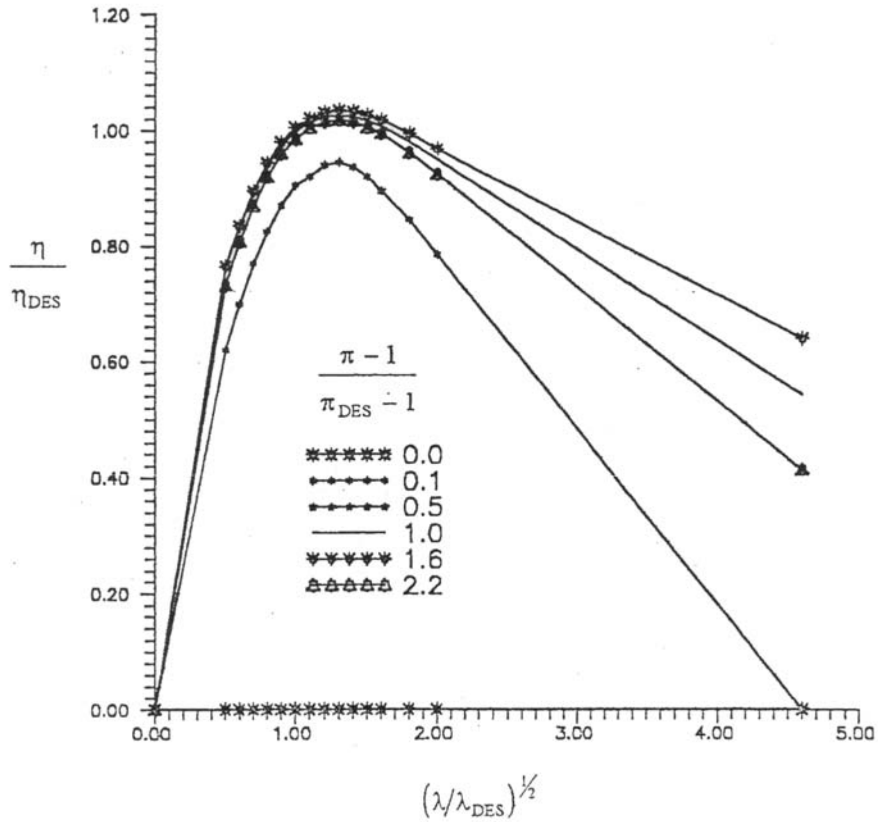

Figure (2.8) Generalized Stage Efficiency Correlation T56-A14 [1]

T56 turbine is modelled normalized flow function is used to model each of the four turbine stages of said T56-A14 turbine. The normalized flow parameter is represented as a function of the stage pressure ratio parameter, PR_S.- 1 , and the stage speed parameter, $N/\sqrt{t}$, both of which have been normalized with recpect to their design point values. The normalizing value for mass flow Q, is called Q^* is the chocked value of, $W\sqrt{t}/p$, defined at the design speed for the stage.

The normalized flow function shown in Figure (2.9) is derived from available operating data for the T56-A14. engine, and represents the characteristic that best models each of the turbine stages. Note that the flow function is chocked and becomes independent of speed at pressure ratios above the stage design point. Temperature drop for stage can be obtained from Figure (2.9) by numerical search given the pressure ratio and the speed.

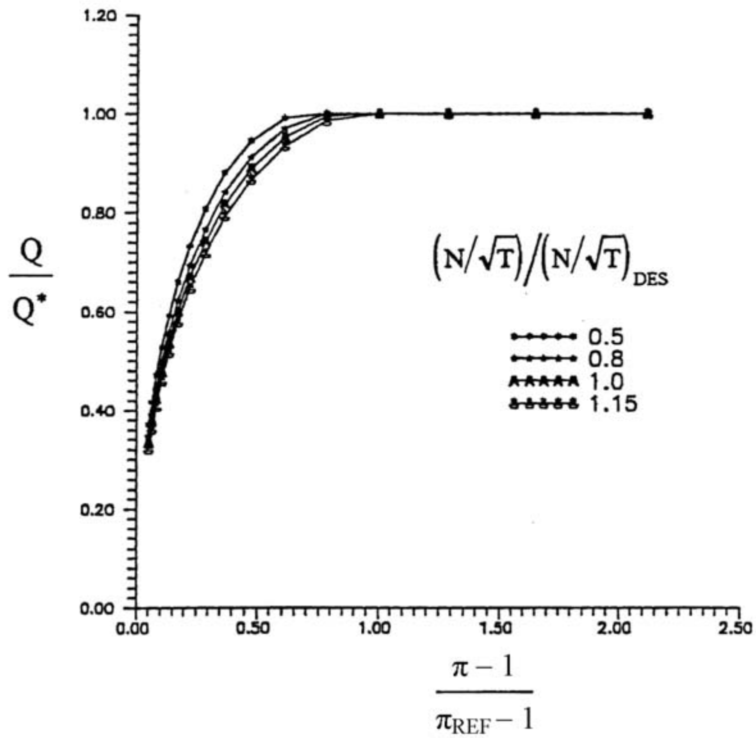

Figure (2.9) Generalized Stage Flow Characteristics T56-A14 [1]

2.4.2 Estimation of Stage Design Point From Overall Design Point

"Estimates of the stage design point, that stage operating parameter at turbine maximum efficieny point is required in order to generate the individual stage performance curves using the generalized flow and efficiency correlations. This estimates convert the single stage turbine data to single turbine stage data. The procedure followed to estimate these parameters from overal turbine design point performance is described as follows"[1]:

1. Assume a relative stage temperature drop split at the design point of the turbine. That is temperature drop of every stage is described (assumed) as a fraction of the overall turbine temperature drop:

$$X_{desi} = \frac{\Delta t_{desi}}{\Delta Tdes} \qquad (2.49)$$

and

$$\sum_{i=1}^{n} X_{desi} = 1.0 \tag{2.50}$$

Then for the i^{th} stage of an n stage turbine the design point temperature drop ratio is given by:

$$\Delta t / t_{desi} = \frac{X_{desi}\left(\Delta T / T\right)_{des}}{1 - \sum_{j=1}^{i-1} X_{desj}\left(\Delta T / T\right)_{des}} \tag{2.51}$$

where $\Delta t / t_{desi} = X_{desi}\left(\Delta T / T\right)_{des}$ (2.52)

2. Perform a multivariable search to determine η_{desi} and PR_{desi} such that:

$$\eta_{desi} = \frac{\left(\Delta t / t\right)_{desi}}{\left[1 - \left(1 / PR_{desi}\right)^{\varepsilon g}\right]} \tag{2.53}$$

and $PR_{des} = \prod_{i=1}^{n} PR_{desi}$ (2.54)

3. Evaluate the design flow coefficient for each stage coefficient as follows:

$$Q_{des\_i} = Q_{des\_i-1} PR_{des} \sqrt{1 - \left(\Delta t / t\right)_{des\_i-1}} \tag{2.55}$$

noting that

$$Q_{des\_i} = Q_{des} \tag{2.56}$$

4. Evaluate the design speed parameter for each stage according to:

$$N / \sqrt{t_{des\_i}} = N / \sqrt{t_{des\_i-1}} \frac{1}{\sqrt{1 - \Delta t / t_{des\_i-1}}} \tag{2.57}$$

The stage performance parameters estimated for T56-A14 for the assumed temparature drop ratio split at design condition are listed at Table(2.2)

Table (2.2) Estimated T56-A14 TurbineDesign Performance.[1]

Stage	$\Delta t / \Delta T$	$N / \sqrt{t}$	PR	Q	$\Delta t / t$	η
1	0.300	280.2	1.69	12.05	0.107	0.878
2	0.267	296.6	1.70	19.20	0.107	0.866
3	0.233	313.9	1.66	30.77	0.105	0.880
4	0.200	331.7	1.62	48.34	0.100	0.887
Overall	--	280.2	7.86	12.05	0.358	0.897

Having evaluated each of the stage design point performance parameters, it is then possible to generate the individual stage characteristics using the normalized flow function and generalized efficiency correlation as described.

Each stage is represented by two characteristics.

1 - $Q_i = f\left(PR_i, N / \sqrt{t_i}\right)$.

2 - $\Delta t / t_i = f\left(PR_i, N / \sqrt{t_i}\right)$

which are used in the series matching process described below.

2.4.3 Series Matching of Turbine Stages

Once the individual stage characteristics have been estimated, the overall turbine map can be synthesized by matching each stage in series. The procedure is identical to the method of matching two or more turbines in series.

Flow compatibility between each turbine stage dictates that the operating point for a stage is in turn determined by the swallowing capacity of the stage directly downstream. For this reason, the matching procedure works backwards, begining with operating points on the last stage's characteristic as described below.

1. Choose a value of corrected speed parameter $N / \sqrt{T}$ for the turbine.
2. Choose a value of stage pressure ratio, PR_n , as applied to the last stage.

3. Guess values of $N/\sqrt{t_i}$ for each stage, noting that the value for the first stage is identical to that for the stage, since t_1 is the turbine inlet temperature.
4. Determine the operating point on the last stages characteristic. This gives initial values of Q_{i+1} and $\Delta t/t_{i+1}$.
5. Using the temperature drop and flow characteristics of stage 'i' directly upstream as well as the compatibility of flow equation, generate values of downstream flow function, Q'_{i+1}, as a fuction of PR_i for the assumed value of $N/\sqrt{t_i}$.

$$Q'_{i+1} = Q_i \cdot PR_i \cdot \sqrt{1-(\Delta t/t)_i} \tag{2.58}$$

6. Determine the pressure ratio, PR_i , for which flow compatibility is satisfied. i.e. when $Q'_{i+1} = Q_{i+1}$
7. Given the pressure ratio PR and the assumed value of $N/\sqrt{t_i}$, determine Q_i and $\Delta t/t_i$ from the stage flow and temperature drop characteristics.
8. Having defined the operating conditions for the current stage, repeat steps 5 to 7 for the next stage, and all subsequent stages.
9. Repeat from step 3 until speed compatibility is achieved.

   i.e, when $$N/\sqrt{t_{i+1}} = N/\sqrt{t_i}\,/\sqrt{1-(\Delta t/t_i)} \tag{2.59}$$

10. Determine the overall performance parameters as follows:

$$Q = Q_1 \tag{2.60}$$

$$PR = \prod_{i=1}^{n} PR_i \tag{2.61}$$

$$\frac{\Delta T}{T} = \left(\frac{\Delta t}{t_1}\right) + \left(\frac{\Delta t}{t_2}\right)\cdot\left(1-\frac{\Delta t}{t_1}\right) + \ldots \tag{2.62}$$

And $$\eta = \frac{\Delta T/T}{\left[1-(1/PR)^{\varepsilon}\right]} \tag{2.63}$$

The above procedure, summerized in Figure (2.12) can be performaned for several turbine speeds and pressure ratios to provide the overal turbine performance map required [2].

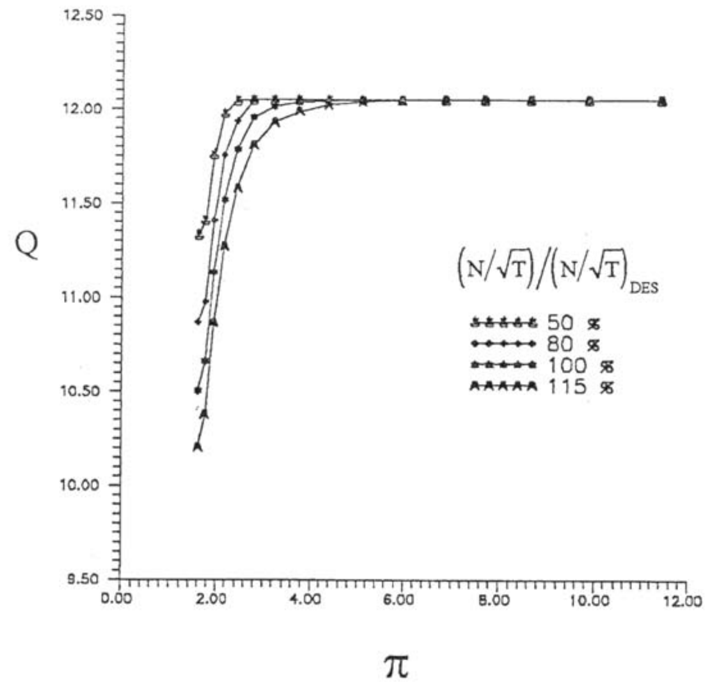

Figure(2.10) Turbine Mass Flow Characteristics.[1]

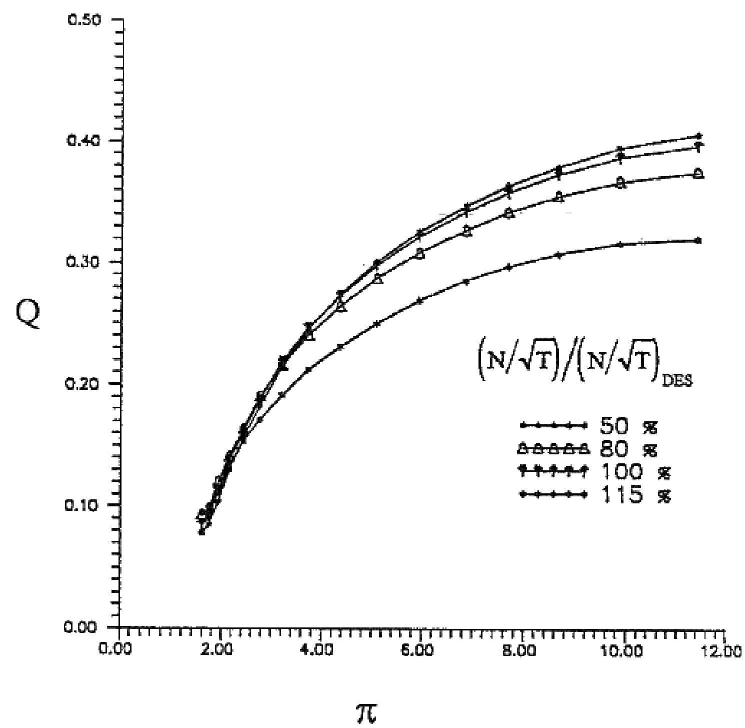

Figure (2.11) Turbine Temperature Drop Characteristics.[1]

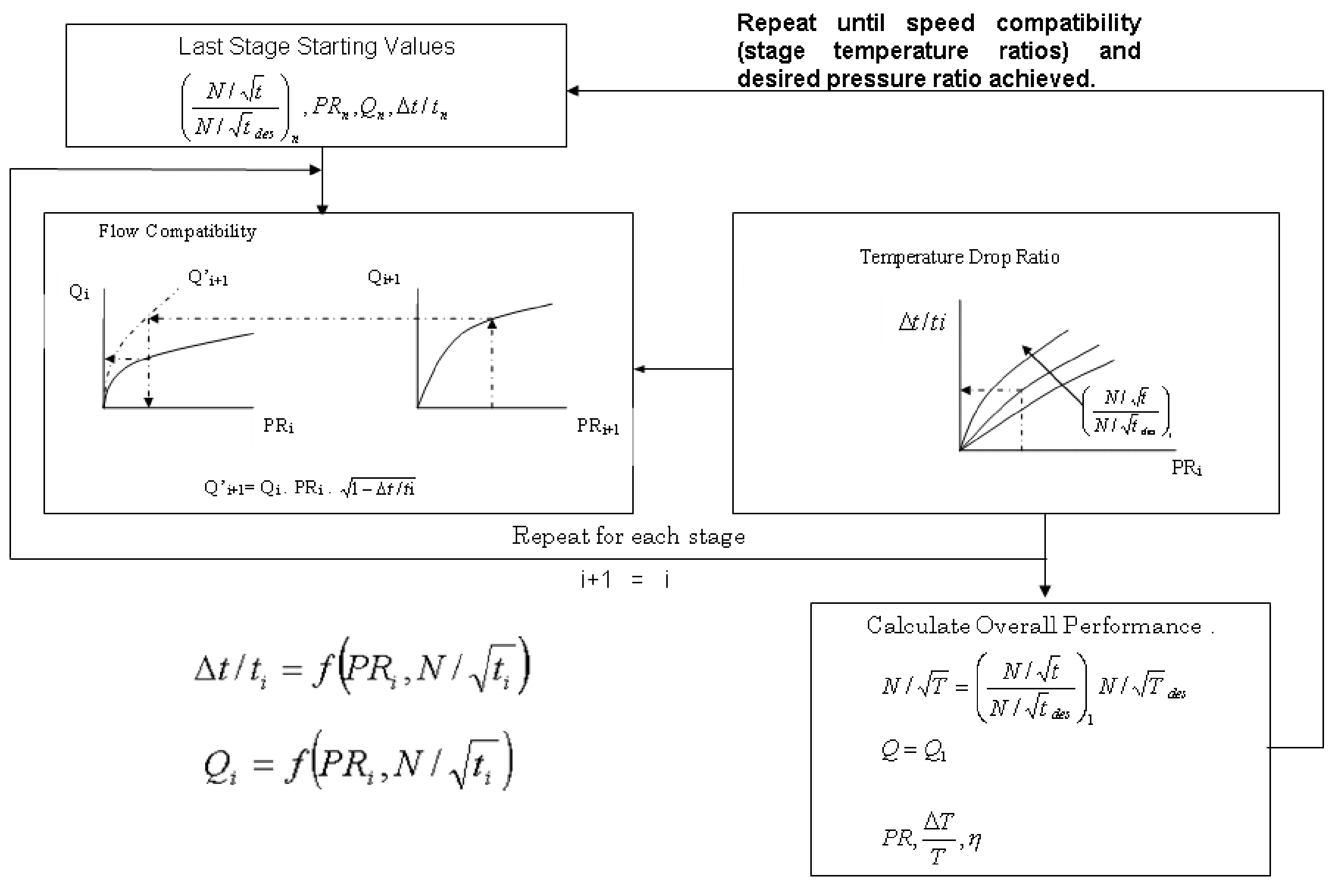

Figure (2.12) Turbine Series Matching Procedure.

CHAPTER 3

COMPONENT MATCHING OF SINGLE SHAFT GAS TURBINE

Variation of performance and fuel consumption over the whole operating range of shaft speed and power output of the gas turbine is off-design performance. Furthermore the results of off-design performance analysis is used to size the engine and its components Off design performance analysis are also used to estimate the limits of the gas generator, invaluable for the mission analysis of the gas turbine.

The procedure applied to obtain overall steady state performance at whole operating range of engine. The procedure is simply satisfying the essantial conditions compatiblity of mass flow, work and rotational speed between the compressor and turbine. The variation of compressor and turbine performance with rotational speed and pressure ratio is obtained using estimated compressor and turbine maps.

The matching program for the Allison T56 engine and Turbo Rotary Compound Engine requires the following inputs for the turbo components.

The performance map data is required to represent the performance characteristics of compressor and the turbine. The compressor characteristics are generally given in terms of non-dimensional quantities of non-dimensional flow $W\sqrt{\theta}/\delta$,total pressure ratio π, corrected speed $N/\sqrt{\theta}$ and total temperature rise $\Delta T/T$. The turbine characteristics are generally given in terms of non-dimensional quantities of non-dimensional flow $W\sqrt{\theta}/\delta$,total pressure ratio π, corrected speed $N/\sqrt{T}$ and total temperature drop $\Delta T/T$. In addition to component characteristics the estimation procedure also requires general constraints tabulated in table (3.1)

Table (3.1) Component Matchig Constraints

Mechanical Constraints	**Equivalent Cycle Parameter**
Gas temperature limit at the turbine rotor inlet	T_4(max.)
Exhaust gas temperature limit.	EGT, T_5 and T_6
Gear box and shaft power limits for turbine output and power extraction.	P_{TO},HP_L(max)
All rotor speeds	N(max.)
Aerothermodynamic constraints	**Equivalent Cycle Parameter**
Maximum rotor speed and flow of each compression component.	$N/\sqrt{\theta}$,$W\sqrt{\theta}/\delta$ (max.)
Stall pressure ratio on axial flow compressor for stall margin on operating line	π_C
Turbine flow fuctions, corrected speed, and expansion and nozzle stability.	$W\sqrt{\theta}/\delta$, $N/\sqrt{\theta}$,PR(max.)

The overall engine model can be obtained by collection of modules. These modules represent the behaviour of the engin components compressor, combustor and the turbine.

3.1 Component Modules

3.1.1 Compressor

The actual performance of compressor can be obtained from set of thermodynamic maps. Using the compressor pressure ratio and corrected speed the values of non-dimensional flow and temperature rise ratio can be obtained from the maps.
(Figure 4.1,4.2)

$$\frac{P_3}{P_4} = f\left(N/\sqrt{\theta}, \frac{W\sqrt{\theta}}{\delta}\right) \tag{3.1}$$

$$\frac{\Delta T}{T} = f\left(N/\sqrt{\theta}, \frac{W\sqrt{\theta}}{\delta}\right) \tag{3.2}$$

The engine inlet pressure loss is evaluated by a simple duct pressure loss relation which use of corrected inlet flow and duct pressure loss coefficient.

$$P_2 = P_a \cdot \left[1 - K_{in}\left(\frac{W_2}{W_1}\right)\right] \tag{3.3}$$

Compressor exit flow, compressor exit temperrature and compressor power extraction can be evaluated using the following relations:

$$W_3 = \left(\frac{W_2 \cdot \sqrt{\theta_2}}{\delta_2}\right) \cdot \left(\frac{P_2}{P_{ref}}\right) \cdot \left(\frac{T_{ref}}{T}\right)^{1/2} \tag{3.4}$$

$$T_3 = \left(\frac{T_3 - T_2}{T_2}\right) \cdot T_2 + T_2 \tag{3.5}$$

$$HP_C = C_{pa} \cdot W_2 \cdot (T_3 - T_2) \tag{3.6}$$

3.1.2 Combustor

The amount of fuel required to raise the temperature of the flow at the compressor exit to turbine inlet temperature which will satisfy the physical match is determined.The computation also takes the pressure loss and thermodynamic properties (3.7,3.8,3.9) into acount.

$$h_{a3} = f(T_3) \tag{3.7}$$

$$h_{a4} = f(T_4) \tag{3.8}$$

$$ECV_4 = f(T_4) \tag{3.9}$$

The fuel ratio is calculated as

$$\frac{W_f}{W_3} = \frac{h_{a4} - h_{a3}}{ECV_4 \cdot \eta_{cc}} \tag{3.10}$$

The pressure loss through combustion chamber

$$P_4 = P_3 \cdot \left[1 - K_{cc} \cdot \left(\frac{W_3 \cdot \sqrt{T_3}}{P_3} \right)^2 \right] \tag{3.11}$$

3.1.1 Turbine

From the turbine performance maps the values of corrected flow and temperature drop ratio can be extracted

$$Q = f\left(N / \sqrt{T}, \pi\right) \tag{3.12}$$

$$\frac{\Delta T}{T} = f\left(N / \sqrt{T}, \pi\right) \tag{3.13}$$

The values of corrected flow, turbine exit pressure and corrected speed. The turbine exit flow, exhaust temperature turbine power and exit pressure calculated.

$$W_4 = \frac{W_4 \cdot \sqrt{T_4}}{P_4} \cdot \frac{P_4}{\sqrt{T_4}} \tag{3.14}$$

$$T_5 = T_4 - \left(\frac{T_4 - T_5}{T_4} \right) \cdot T_4 \tag{3.15}$$

$$HP_t = C_{PG} \cdot W_4 \cdot \left(T_4 - T_5\right) \tag{3.16}$$

The axial turbine is assumed to be chocked at a single corrected value. This is in agreement with the generally accepted off-design performance calculation procedure.

3.2 Cost Function

In order to achieve steady state operation of a single spool at a given inlet rotor speed and engine inlet conditions its necessary to maintain a balance of flow between the compressor and its driving turbine.

$$W_3 - W_f - W_4 = 0 \tag{3.20}$$

A different component matching condition for each load level determined by the compatibility of power relation:

$$(\eta_m HP_t - HP_c)\eta_{gb} - HP_L = 0 \tag{3.21}$$

Then an error (cost) function for a given load level and inlet conditions is:

$$F(E) = E_1^2 + E_2^2 + PF \tag{3.22}$$

The penalty factor (PF) is added into cost, to prevent the solution violate the constraints.

where $E_1 = W_3 + W_f - W_4$ (3.23)

$E_2 = (\eta_m HP_t - HP_c)\eta_{gb} - HP_L$ (3.24)

may be used to define a valid component match. That is,

$$F(E) = E_1^2 + E_2^2 = 0 \tag{3.25}$$

Furthermore, since each power level results in a unique set of engine performance parameters, the error function may be generally formulated as :

$F(E) = E_1^2 + E_2^2 + PF$ (3.26)

where $E_1 = W_3 + W_f - W_4$ (3.27)

E_2 = (Parameter) – (Parameter Desired) and the match point may be evaluated for any performance parameter required turbine inlet temperature , power level.. etc.

For a single-shaft simple cycle engine, If the compressor delivery pressure, P_3 and the turbine inlet temperature,T_4 , are guessed, then each then each of the error terms can be evaluated. In other words

$$F(E) = f(P_3, T_4) \tag{3.28}$$

and the matching task becomes one of finding the values of P_3 and T_4 such that

$$F(E)=0. \tag{3.29}$$

The cost function for the compatibility of the turbo-rotary compound engine components is similar, the number of independent variables and error terms are doubled.

$$F(E) = E_1^2 + E_2^2 + E_3^2 + E_4^2 + PF \tag{3.30}$$

where $E_1 = W_3 + W_f - W_4'$ (3.31)

$$E_3 = W_3' + W_f - W_4 \tag{3.32}$$

E_2 = (Parameter) – (Parameter Desired)

E_4 = (Parameter) – (Parameter Desired)

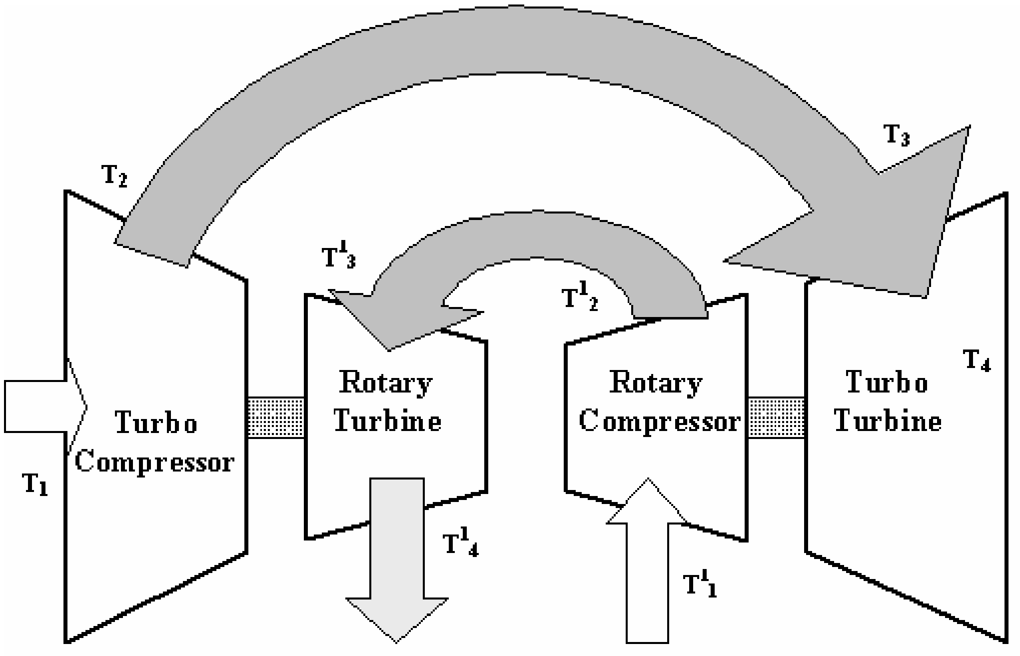

Figure (3.1) Flow Chart of TURC engine

Note that in case of power compatibility the flow and shafts are cross coupled.
that

$$E_2 = \left(\eta_m HP_t' - HP_c\right)\eta_{gb} - HP_L \tag{3.33}$$

$$E_4 = \left(\eta_m HP_t - HP_c'\right)\eta_{gb} - HP_L \tag{3.34}$$

3.3 Overall Performance Parameters

After each matching procedure is completed all parameters are calculated, the overall performance parameters calculated as follows [1]

Compressor Efficiency

$$\eta_c = \frac{\left[\left(P_3 / P_2\right)^{\frac{(\gamma_c - 1)}{\gamma_c}} - 1\right]}{\Delta T / T_2} \tag{3.17}$$

Turbine Efficiency

$$\eta_t = \frac{\Delta T / T_4}{\left[\left(P_4 / P_3 \right)^{\frac{(\gamma_t - 1)}{\gamma_t}} - 1 \right]} \tag{3.18}$$

Net power or Load power

$$HP_L = \left(\eta_M HP_T - HP_C \right) \cdot \eta_{GB} \tag{3.18}$$

Specific Fuel Consumption

$$SFC = \frac{W_F}{HP_L} \tag{3.19}$$

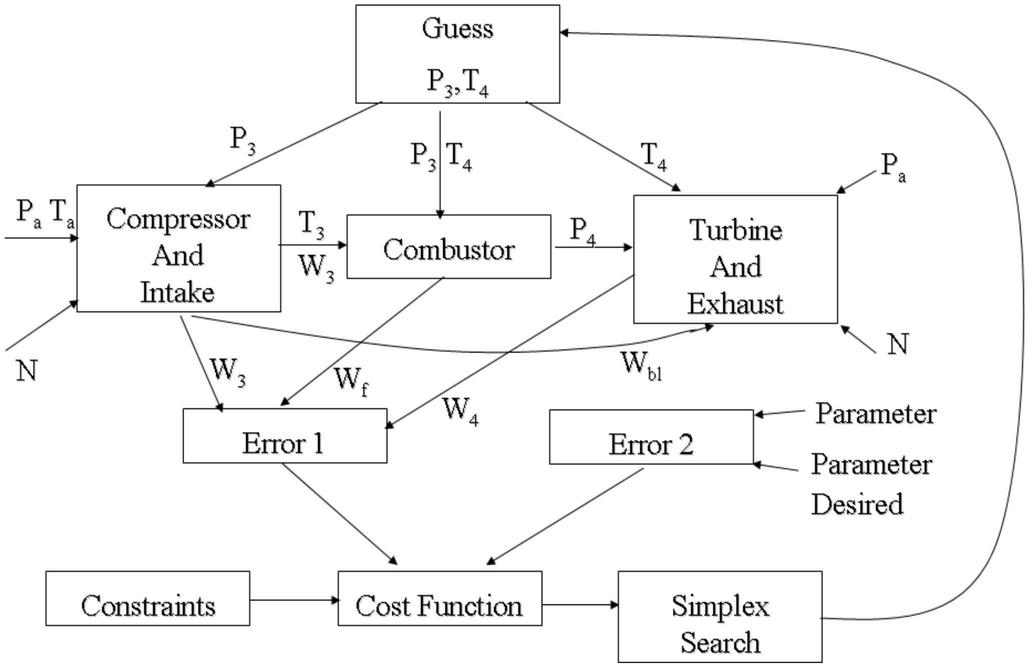

Figure (3.2) T56-A14 Component Matching

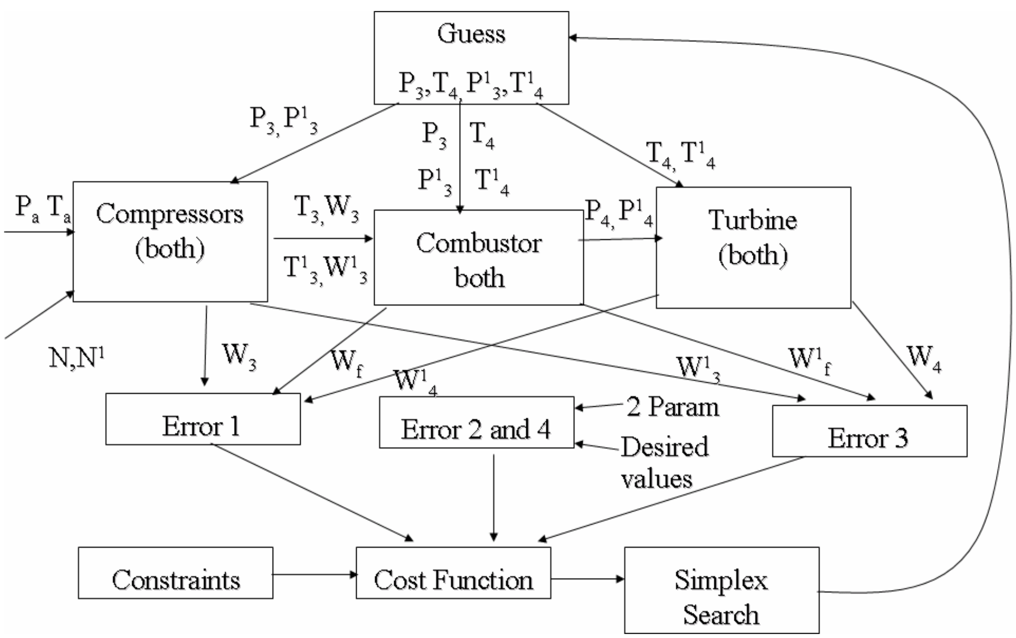

Figure (3.3) TURC Component Matching

CHAPTER 4

NUMERICAL RESULTS

The main aim of this chapter is to demonstrate the results of overall performance estimations of T56-A14 and the hybrid engine TURC comparatively. Also the results of the turbo components compressor and turbine performance map estimation models build using the same procedure with Reference [1], [2] are presented. The results can be compared with the results of References.

In this study, the design speed of both positive displacement type rotary compressor and turbine are taken as and the components are sized to fit the axial turbine and compressor, such that an internal mass flow of 5-15 kg/sec can be accommodated through the positive displacement components. Losses in axial and rotary components are only accounted through respective component efficiencies. Accordingly the rotary compressor polytropic efficiency is taken as 0.921 and the rotary turbine polytropic efficiency is taken to be 0.907.

4.1 Compressor Performance Estimation Results

The Figures (4.1) and (4.2) display resulting T56-A14 compressor pressure ratio and temperature rise characteristics with respect to mass flow parameter for speed range between %82-107.

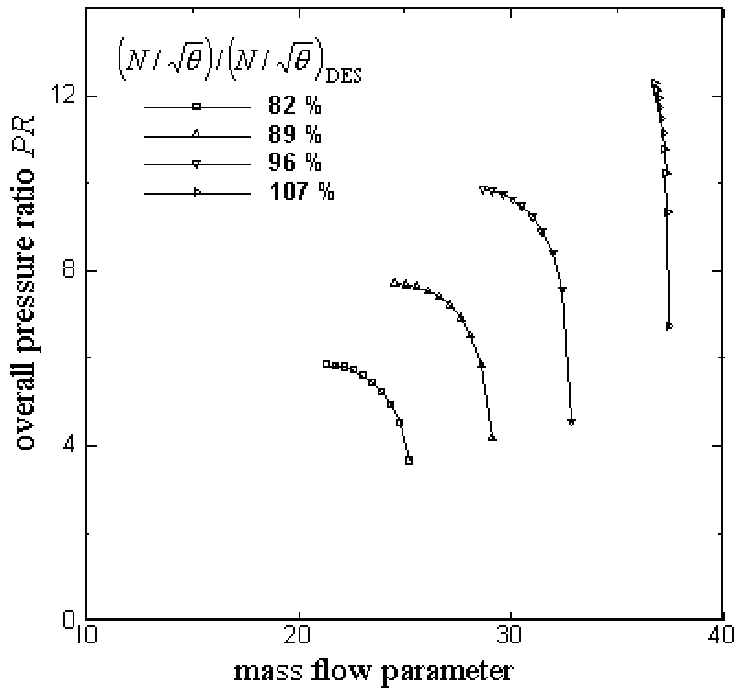

Figure (4.1) Overall Pressure Rise Characteristics.

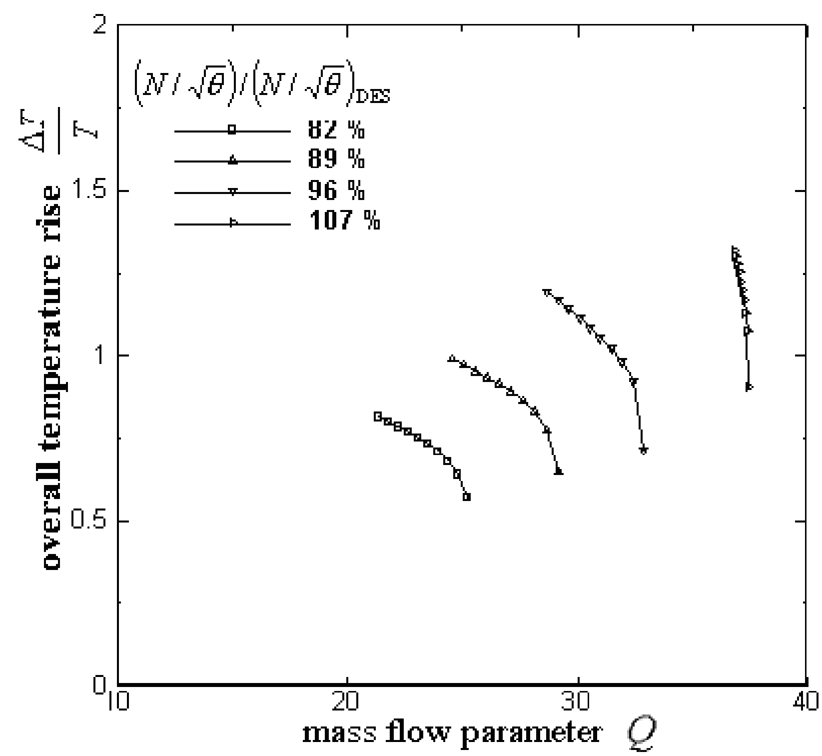

Figure (4.2) Overall Temperature Rise Characteristics.

4.2. Turbine Performance Estimation Results

The Figures (4.3) and (4.4) display resulting T56-A14 turbine mass flow and temperature drop characteristics with respect to pressure ratio for speed range between %82-121.

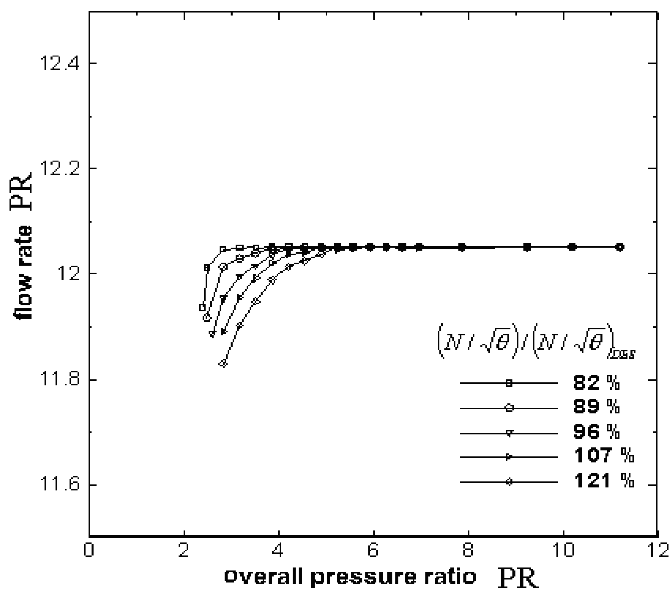

Figure (4.3) Turbine Overall Flow Characteristics.

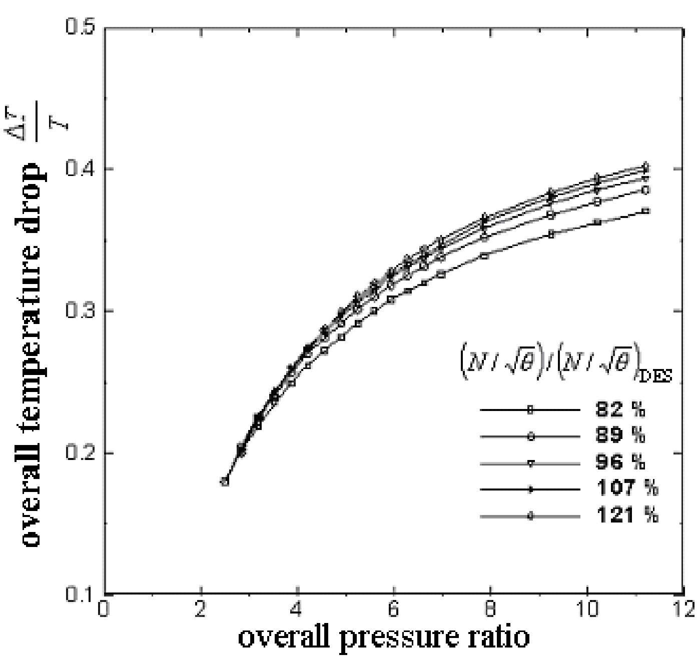

Figure (4.4) Turbine Overall Temperature Drop Characteristics

4.3. Engine Performance Characteristics

The pumping characteristics obtained by matching Figures (4.5),(4.6) and (4.7) show how the performance of an engine changes with rotational speed. Figure (4.5) exhibits the behavior of a typical T56-A14 engine serving as a baseline to the new TuRC engine. Those for the compound engine ae tabulated in Figures (4.6) and (4.7).

The results are consistent with those published by Kerrebrock [32] We see that the specific fuel consumption decreases as rotational speed increases, as the speed approach the design point 13850rpm. This is because the relative percentage of work energy input, that the compressor pressure ratio is increasing. $TTR = T_{t5} / T_{t0}$ is the exit-to-inlet total temperature ratio. Its value remains relatively high at almost all speeds, indicating a high engine exhaust heat rate and a low thermal efficiency. Exit-to-inlet pressure ratio $PTR = P_{t5} / P_{t0}$ and relative mass flow rate ratio $\dot{m} / \dot{m}_{design}$ do increase with rotational speed as expected.

When these results are compared with those obtained for the turbo-rotary compound engine (Figure 4.6), it is seen that the specific fuel consumption has improved by %37 for the lower corrected speeds and by %20 for the higher corrected speeds. The compound engine also demonstrate the characteristics of internal combustion engine (higher efficiency). This performance improvement can also be followed from the turbine exit temperature –or exhaust heat rate- which has been reduced by more that 30% for all speeds. As for the total pressure ratio $PTR = P_{t5} / P_{t0}$ and primary mass flow $\dot{m} / \dot{m}_{design}$ across the engines, there are no big differences between baseline T56 engine and TuRC engine. The pumping characteristics belonging to the secondary stream that passes through the rotary compressor and the rotary turbine is given in Figure (4.7). The very low exit to inlet $TTR = T_{t5} / T_{t0}$ total temperature ratio attests to the very efficient power extraction process that occurs within the rotary turbine. Actually, the rotary turbine inlet temperature was kept at 1700°F to minimize any cooling requirements. Actually, rotary turbine requires much less cooling because it partly cools itself during its own expansion. The periodic firing outside and within the turbine would therefore allow for an operation at much higher inlet temperatures. The direct benefit of running at higher temperatures would directly reflect itself in the size decrease of rotary components. In that sense, it is safe to say that the relative size of rotary components in the present work is much bigger than what it would have been in reality. An unsteady rotary turbine inlet temperature increase by 700°F, would roughly decrease the required rotary component volume by more than 40%.

The overall specific consumption which is the ratio of the fuel consumed for turbo (SFC) and rotary (RSFC) components have been given separately in Figures (4.6) and (4.7) the total net power produced by the compound engine for the calculation of SFC since the front spool does not produce extra power.

The overall specific consumption which is the ratio of the total fuel consumed and the net power produced by the TuRC engine is given in Figure (4.7). The impressive decrease in specific fuel consumption of the TuRC engine can be attributed to two sources. The first part of the lower SFC comes from the energy saved, achieved by draining less axial turbine power during the closed volume rotary compression phase. The second part of a lower SFC comes from the longer expansion phase of the rotary turbine which is thus able to extract more power from combusted gas. Hence more net energy is achieved at the end of the compound cycle.

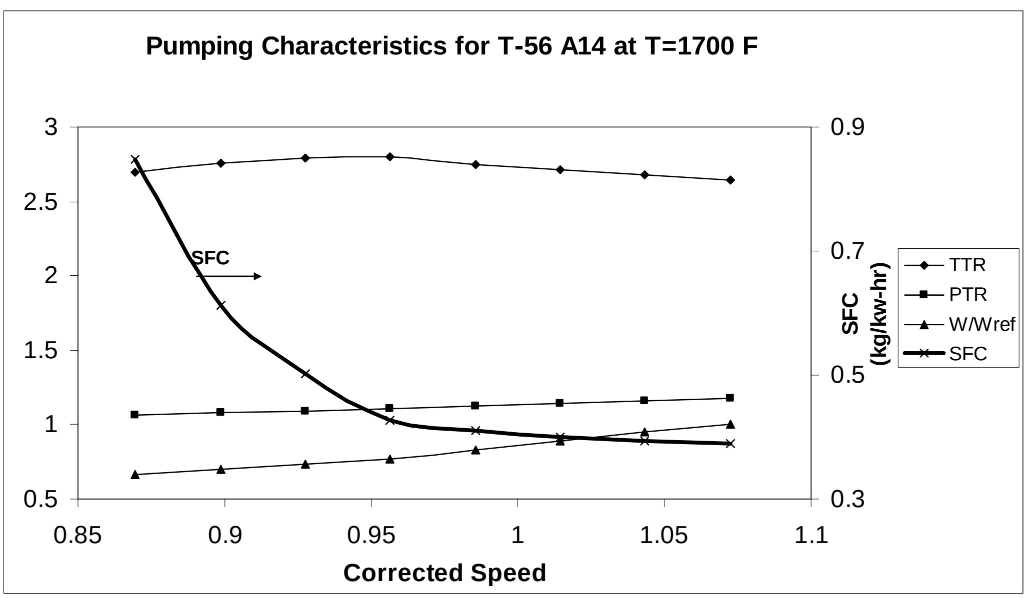

Figure (4.5) Pumping Characteristics of Baseline T56-A14 Engine

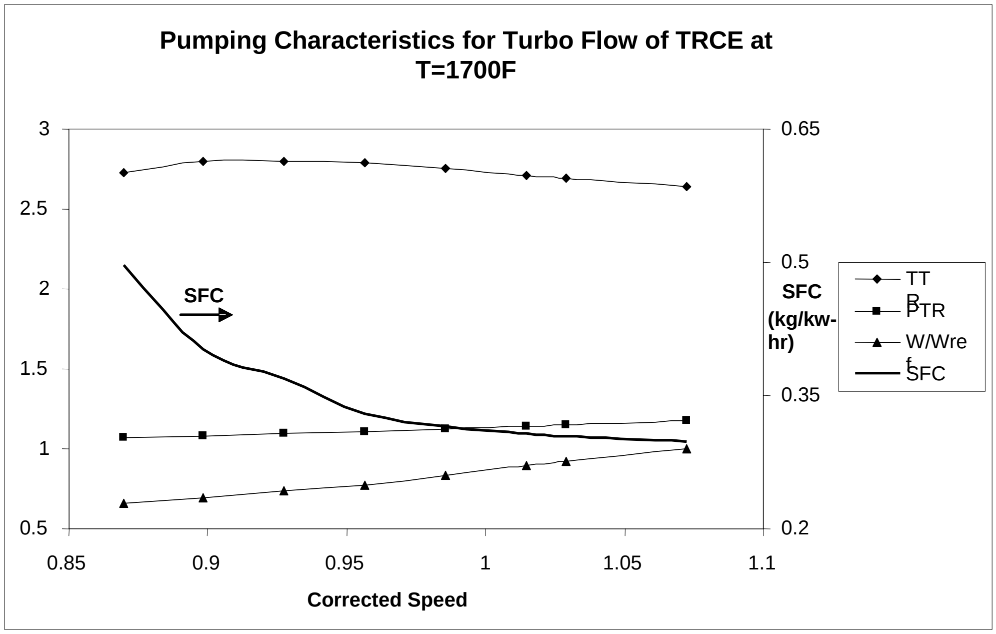

Figure (4.6) Pumping Characteristics of TURC Primary Flow Passing Through Turbo Compressor and Turbine

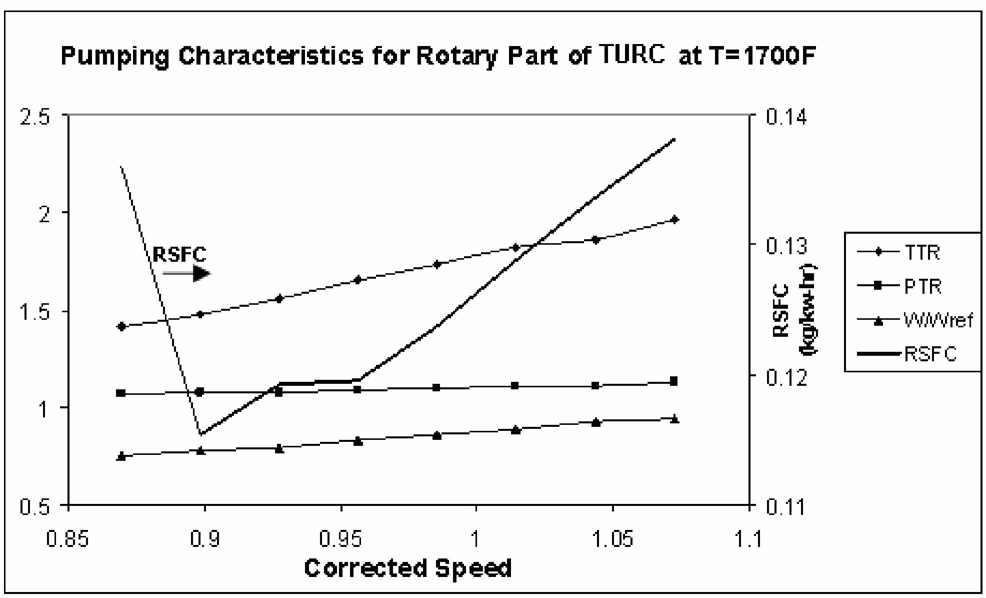

Figure (4.7) Pumping Characteristics of TURC Secondary Flow Passing Through Rotary Compressor and Turbine

The performance maps given in Figure (4.8) and Figure.(4.9) clearly show the improvement in specific fuel consumption and power obtained when rotary components are integrated within a gas turbine engine. The main design philosophy of the TuRC engine is the minimization of the energy used internally by the engine components. Among all others, compressor is the biggest shaft energy consumer. The energy supplied to the compressor is huge because it often exceeds 50% of the chemical energy input within the combustion chamber. This huge shaft power supplied to the compressor cannot be decreased because the steady flow compression process is achieved as both ends of the compressor are to be kept open at all time to allow steady flow in and out of the compression volume. Rotary compressors, partially alleviate this problem as they provide an efficient and cheaper compression process for the secondary flow that serves the internal power needs of the engine. This energy saving of around 30% reflects in the following performance map (Figure 4.9), almost for all rotational speeds and compressor pressure ratios.

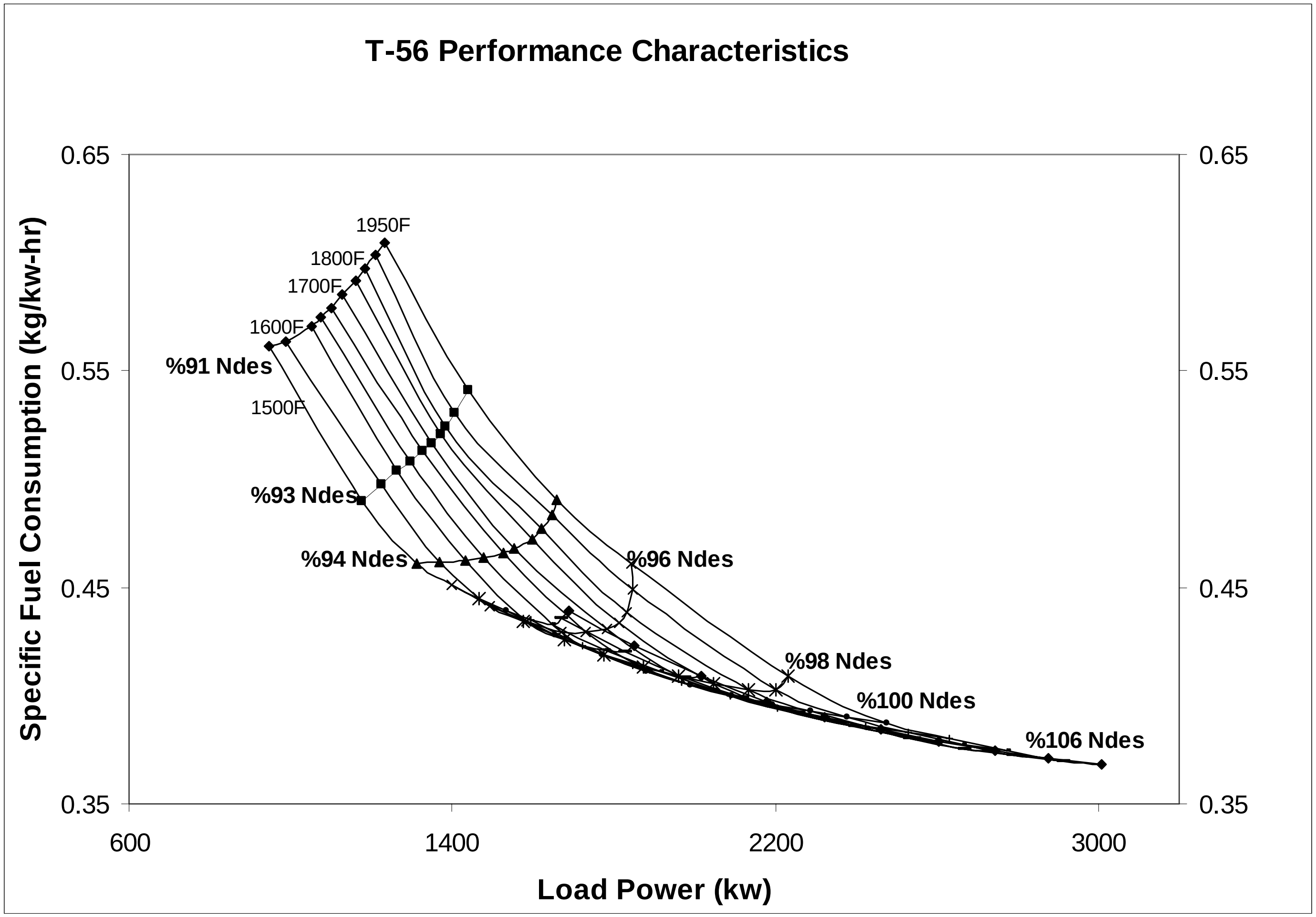

Figure (4.8) Performance Map of Baseline T56-A14 Turboprop Engine

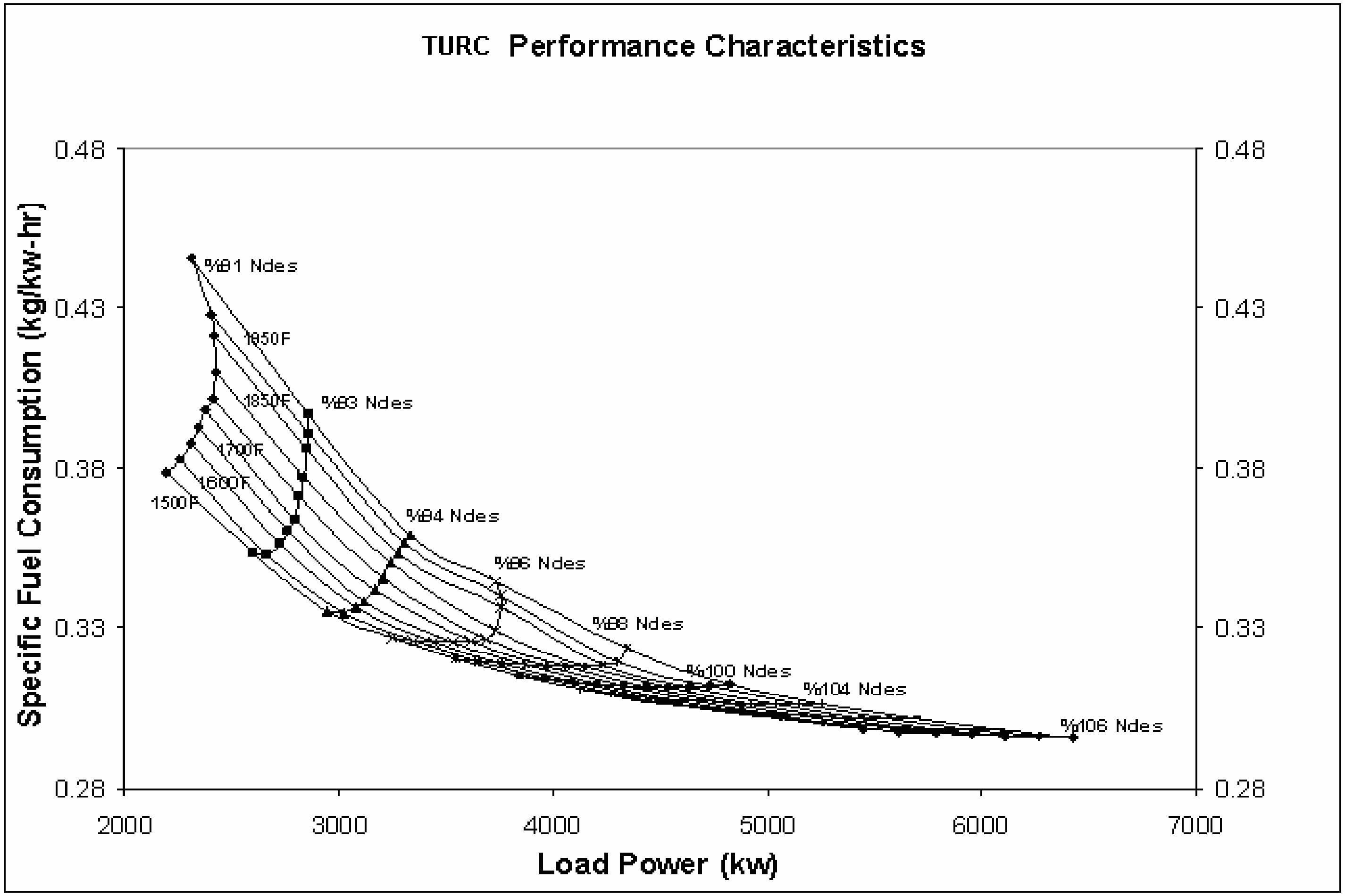

Figure (4.9) Performance Map of Turbo Rotary Compound Engine (TURC)

CHAPTER 5

CONCLUSION

The study analyzes the steady state performance prediction of two different axial flow gas turbine engines and presents new computer codes for steady state uninstalled performance simulation of a single spool turbojet and separate spool compound engine. The aim is to compare the performance characteristics of a gas turbine engines.

The simulation methods have been applied to the Allison T56 and the new concept engine Turbo Rotary Compound Engine. The models are component matching based programs simulating the engines over a wide range of operating conditions.

The component performance maps that are required for performance modeling of turbo components axial flow compressor and turbine have been obtained [1], [2].

The off design performance characteristics of axial compressor is obtained by stage stacking method. A stage level modeling method based on meanline stage stacking analysis has been established, to generate the compressor performance map. The T56-A14 axial compressor gas path geometry and generalized stage characteristics (Figure 2.3) were obtained from the presented curves in Reference [1]. The estimated performance map of the computer program is as expected. As the mass flow is reduced at fixed speed the pressure ratio rises until limiting value ("stall line") At low corrected speeds the pressure ratio change considerably with mass flow rate.

To generate the turbine performance maps the turbine stage characteristics have been synthesized by the series matching technique. Usually turbine is choked at a single corrected flow value over the entire operational range.

The performance map results obtained are in agreement with the verified off-design performance calculation results with Reference [1].

The matching results obtained searching component operating points for speed work and flow compatibility are tabulated in the Figure.(4.5), (4.6) and (4.7) as pumping characteristics of the engines for fixed turbine inlet temperature at 1700 F.

The decrease in SFC (specific fuel consumption) for TURC engine is not surprising since nearly half (i.e. Figure 4.5 and 4.6 W/W_{ref}) of flow is passing through an almost ideally expanding (i.e. Figure 4.5 and 4.6 PR) internal combustion process.

As a result, the power budget left for free power or thrust generation is almost doubled. TURC engine being almost the same size as the T56-A14, produces twice as much power as this well known conventional engine. TURC engine succeeds in delivering high power and high engine efficiency, all at the same time. When looked from this side, it is not unrealistic to say that TURC engine extends the high thrust, high efficiency performance characteristics of high power turbofan engines down to medium-to-small size turbo engines.

REFERENCES

[1] "Computer Model of the T56 Turboprop engine: Thermodynamic Analysis and System Design", GasTOPS Ltd., GTL-TR-19-22.1.1,1984.

[2] Arslanoğlu M., "Simulation of Axial Flow Aircraft Engines for Steady State Performance Prediction and Fault Diagnostics", M.Sc. Thesis, Department of Aeronautical Engineering, Middle East Thecnical University, August 2005

[3] Mattingly J. D., "Elements of Gas Turbine Propulsion", McGraw-Hill International Edition, Singapore, 1996.

[4] Akmandor I. S., Ercan T., Karaca, " Turbo Rotary Compound Engine and Novel Thermodynamic Cycle", ASME Turbo Expo 2005, June 6-9, 2005, Reno-Tahoe, Nevada, USA

[5] Arslanoğlu M., Göğüş Y., Akmandor I. Sinan, Güneş Erdoğan, Bird Jeff W. "A Component Based Modelling Method for Steady State Performance Prediction and Diagnostics of Gas Turbines".

[6] Çengel Yunus A., Boles Micheal A., "Thermodynamic An Engineering Approach", Mc Graw Hill, 1989.

[7] Ganesan V., "Internal Combustion Engines", Mc-Graw Hill, 1994

[8] Heywood John B., "Internal Combustion Engines", McGraw-Hill International Edition, 1988.

[9] I.S. Akmandor , T. Ercan, M. Karaca, G. Aran, “New Engine and Thermodynamic Cycle of Tusas Aerospace Industries (TAI) Unmanned Air Vehicle” International Symposium on Innovative Aerial/Space Flyer Systems, ISIASFS PL-11, Series on Mechanical System Innovation- The University of Tokyo, Japan, 2004

[10] Smith D.G. and Rudge, P.G., “Pressure-Volume Diagrams for Sliding Vane Rotary Compressors”, Proc. Instn. Mech. Engineers, Vol.184 Pt3R, 1970.

[11] Chou, Y., “Rotary Vane Engine”, United States Patent Office 5,352,295, October 4th 1994.

[12] Vading, K., “Rotary-Piston Machine”, PCT WO 02/31318, April 18th 2002.

[13] Umeda, S., “Rotary Internal Combustion Engine”, United States Patent Office United States Patent Office 4,414,938, (November 15th 1983).

[14] LAI, J.H., “Stage Combustion Rotary Engine”, United States Patent Office United States Patent Office 5,596,963, (January 28th 1997).

[15] Jirnov, A., and Jirnov, O., “Sliding-Blade Heat Engine with Vortex Combustion Chamber”, United States Patent Office United States Patent Office 5,511,525, (April 30th 1996).

[16] Ray E. Budinger; Harold R. Kaufman, “Investigation of the Performance of a Turbojet Engine with Variable-position Compressor Inlet Guide Vanes”, NACA RM E54L23a, 1955.

[17] F. Corchedi; G. R. Wood, “Design and Development of a 12:1 Pressure Ratio Compressor for the Ruston 6-MW Gas Turbine”, ASME 82-GT-20.

[18] T. F. Balsa; G. L. Mellor, “The Simulation of Axial Compressor Performance Using an Annulus Wall Boundary Layer Theory”, ASME 74-GT-56

[19] E.J. Milner; F. J. Dugan, “Performance of J85-13 Compressor with Clean and Distorted Inlet Flow”, NASA TMX-3304, 1955.

[20] Howell A. R., Bonham R. P., “Overall and Stage Characteristics of Axial Flow Compressors”, Proc. Inst. Mech. Engrs., 1950

[21] Robins W. H., Dugan F. J., “Prediction of Off-design Performance Using an Annulus Wall Boundary Layer Theory”, NASA SP-36, 1965.

[22] Stone A., “Effects of Stage Characteristics and Matching on Axial Flow Compressor Performance”, Transaction of American Society of Mechanical Engineers, 1958.

[23] Doyle M. D., Dixon S. L., “ The Stacking of Compressor Stage Characteristics to Give an Overall Performance Map”, Aeronautical Quarterly, 1962.

[24] Howel A. R., W. J. Calvert, “A New Stage Stacking Technique for Axial Flow Compressor Performance Prediction”, ASME 78-GT-139, 1978.

[25] Horloch, J.H., “ A Rapid Method for Calculating the Off-design Performance of Compressor and Turbines”, Aero. Quarterly, 1958.

[26] Ainley D.G. and Mathieson G.C.R., “A Method of Performance Estimation for Axial Flow Turbines”, Aero Res. Council Rep. and Memo, 1957.

[27] Akmandor, I. S. and Ersöz, N., “Compound and Single Use of Rotary Vane Engine and Thermodynamic Cycle”, International Patent Application No.

PCT/TR03/00071, WIPO, September 9th, 2003.

[28] Akmandor, I. S. and Ersöz, N., “Compound and Single Use of Rotary Vane Engine and Thermodynamic Cycle”, International Patent Application No. PCT/TR03/00071, WIPO, September 9th, 2003.

[29] Cohen H., Rogers G.F.C., and Saravanamutto H.I.H., “ Gas Turbine Theory”, Longman Scientific and Technical Publications”, Pearson Education, 2001.

[30] Kurzke J., Riegler C., “A New Compressor Map Scaling Procedure for Preliminary Conceptional Design of Gas Turbines”, Turbo Expo 2000, 8-11 May, Munich, 2000-GT-006

[31] MacIsaac B.D., Saravanamutto H.I.H., “Thermodynamic Models for Pipeline Gas Turbine Diagnostics”, Trans of ASME, 1983.

[32] Kerrebrock, J.L., “Aircraft Engine and Gas Turbines”, The MIT Press, June 1992.

APPENDIX A

SIMPLEX SEARCH

Reference [2] explains the simplex search method as follows: Simplex method is a multi variable optimization method for minimization of n variables. Simplex method is a search method attempting to reduce the value of the cost function by the use of tests near to an estimate of the solutions. The simplex search method determines the direction of search progress in an n dimensional search problem using n+1 observations at mutual equidistant points in the domain which are called simplex vertices. Figure(A.1) is a visual representation of one step of simplex search. In two dimension these observations are made at the vertices of an equilateral triangle, called simplex vertices. The cost function is evaluated at these vertices and the point of maximum cost reflected.

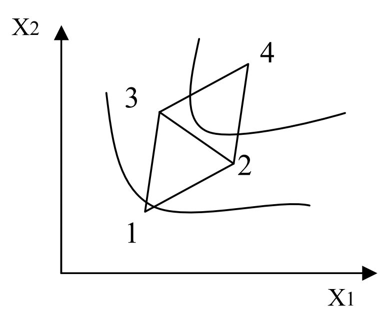

Figure(A.1) Local exploration for the simplex search technique.

In figure a single step of simplex search method in two dimension is demonstrated. The points indicated by are initial simplex vertices. Value of the cost function for simplex “1” is larger then the simplex vertices, is therefore reflected about the remaining vertices 2 and 3 to give new point 4 form the new simplex triangle 2,3 and 4.

Input for the simplex search routine is the cost function to be minimized and the first approximations of the independent variables must be specified at the beginning of the search. Also step size is needed to be specified. As the minimum of the function approached the step size be specified. The search can then be terminated when the step size falls below a specified minimum value.

For simplex search the step size is replaced by a single value which gives the length of one side of simplex. The use of equal units in each dimension points to the importance of correct scaling for this search method. A lower limit to the length of a simplex side is also required so that the search can be terminated.

The progress of the two dimensional search shown in Figure (A.2) will be used to illustrate the search procedure and to demonstrate the action taken when the search oscillates. It is then natural to introduce a contraction of the size of the simplex in order to overcome one of the modes of oscillation.

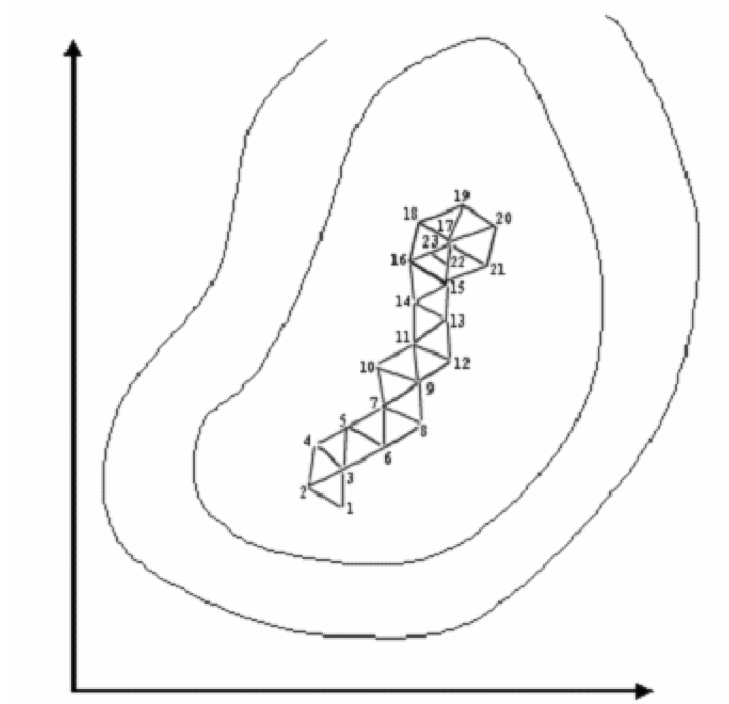

Figure (A.2) The simplex search technique.

The first simplex in Figure (A.2), an equilateral triangle in two dimensions, is defined by the vertices numbered 1,2, and 3.Vertex 1 represents the first approximation to the minimum. The equilateral triangle 1,2,3 is constructed with its side set equal to a specified length. The contours show in this case that reflection is required about the line that joins vertices 2 and 3. Point 4 is then generated and the function evaluated at that point. Since the contours show that the next predicted point is back at vertex 1, the first mode of oscillation has occurred. This situation can be recognized as occurring when the most recently introduced point gives a maximum value of the function and is therefore rejected.

The solution in this situation is quite straightforward. Instead of rejecting vertex 4, the vertex with the second largest function value is rejected. The solution in this situation is quite straightforward. Instead of rejecting vertex 4, the vertex with the second largest function value is rejected. In this case, therefore, vertex 2 is rejected and reflection takes place about the vertices 3 and 4. The search then progresses down the valley until at vertex 17 a second type of oscillation occurs In this case the triangles rotate about one vertex until eventually the search returns to the triangle 15,16 and 17. In n dimensions exact correspondence does not occur due to machine rounding error. Detection of this oscillation must therefore rely on the fact that one vertex of a simplex is used repeatedly.

As soon as this oscillation detected, the size of the simplex is contracted by a factor ½ while the vertex on which the rotation is based is retained. In Figure (A.2), therefore, a new triangle with vertices 17, 22, and 23 is generated and tested. The next vertex, 24, is very close to minimum and several successive rotations and contractions can be expected before the search is terminated when the simplex has shrunk below the size specified. Rotational oscillations of this type are characteristic either when the search is close to minimum, or a narrow valley is nearby. In either case contraction in size is necessary to resolve the direction of movement required.